

# DIAMONDOIDS AND BIOMARKERS IN OIL FROM SAN JOAQUIN BASIN AND SANTA BARBARA BASIN, SOUTHERN CALIFORNIA

Monporn Mesdakom<sup>1</sup>, Kruawun Jankaew<sup>1</sup>, J. Michael Moldowan<sup>2</sup>, and David A. Zinniker<sup>2</sup>

<sup>1</sup>Department of Geology, Faculty of Science, Chulalongkorn University

<sup>2</sup>Department of Geological and Environmental Science, Stanford University

Tel: 086-1258439, e-mail: monpornm@gmail.com

---

## Abstract

This research focused on analyzing diamondoids and biomarkers in oils from the San Joaquin and Santa Barbara Basins. These archived samples provide an opportunity to identify mixed petroleum sources in these well-explored basins allowing for the discovery of possible previously unrecognized cracked oil inputs from deeper sources. Standard solutions and Gas Chromatography-Mass Spectrometry (GCMS) were used to identify compounds (diamondoids and biomarkers) and calculate their concentrations. Diamondoid analyses from 89 samples indicate that 42 (18+24) samples are uncracked oils with low diamondoid concentrations. Higher diamondoid concentrations indicate that 38 (24+14) samples are mixed oils with dominant slightly cracked sources and 9 (5+4) samples are mixed oils with dominant intensely cracked sources. Biomarker analyses suggest that the San Joaquin and Santa Barbara Basins source rocks were likely deposited in hypersaline continental shelf and continental slope with significant plankton inputs, respectively. In conclusion, both basins oils are of relatively moderate to high maturity, varied in biodegradation ranks and generated by multiple source rocks (Cretaceous, Paleogene and Neogene).

**Keywords:** diamondoid, biomarker, cracked oil, uncracked oil

## Acknowledgement

This research would not have been accomplished if I did not get any suggestions, encouragement and support from many people. Firstly, I would like to sincerely thank the Summer Undergraduate Research in Geoscience and Engineering (SURGE) Program, Stanford University for providing an invaluable experience to me to do this research with top-class professors and facilities. Secondly, I appreciate support from Dr. Kruawun Jankaew, Professor J. Michael Moldowan and David A. Zinniker, my advisors, for giving me great suggestions and attitudes. Acknowledgement is also given to PTT Exploration and Production Public Company Limited (PTTEP) for supporting me with a scholarship and spending money to go to Stanford University.

Moreover, I would like to deeply thank to all teachers in the Department of Geology, Faculty of Science, Chulalongkorn University for untiringly giving me knowledge, useful and valuable experience and suggestions for all 4 years of my study.

Lastly, I would like to thank my lovely family, all my very good geology friends and juniors for their kindness and cheerfulness all the time.

# DIAMONDOIDS AND BIOMARKERS IN OIL FROM SAN JOAQUIN BASIN AND SANTA BARBARA BASIN, SOUTHERN CALIFORNIA

Monporn Mesdakom<sup>1</sup>, Kruawun Jankaew<sup>1</sup>, J. Michael Moldowan<sup>2</sup>, and David A. Zinniker<sup>2</sup>

<sup>1</sup>Department of Geology, Faculty of Science, Chulalongkorn University

<sup>2</sup>Department of Geological and Environmental Science, Stanford University

Tel: 086-1258439, e-mail: monpornm@gmail.com

---

## Abstract

This research focused on analyzing diamondoids and biomarkers in oils from the San Joaquin and Santa Barbara Basins. These archived samples provide an opportunity to identify mixed petroleum sources in these well-explored basins allowing for the discovery of possible previously unrecognized cracked oil inputs from deeper sources. Standard solutions and Gas Chromatography-Mass Spectrometry (GCMS) were used to identify compounds (diamondoids and biomarkers) and calculate their concentrations. Diamondoid analyses from 89 samples indicate that 42 (18+24) samples are uncracked oils with low diamondoid concentrations. Higher diamondoid concentrations indicate that 38 (24+14) samples are mixed oils with dominant slightly cracked sources and 9 (5+4) samples are mixed oils with dominant intensely cracked sources. Biomarker analyses suggest that the San Joaquin and Santa Barbara Basins source rocks were likely deposited in hypersaline continental shelf and continental slope with significant plankton inputs, respectively. In conclusion, both basins oils are of relatively moderate to high maturity, varied in biodegradation ranks and generated by multiple source rocks (Cretaceous, Paleogene and Neogene).

**Keywords:** diamondoid, biomarker, cracked oil, uncracked oil

# ไดอะมอนดอยด์และไบโอมาร์กเกอร์ในน้ำมันจากแองซาน ไฮควิน และแองซานต้า บาร์บารา บริเวณทางตอนใต้ของรัฐแคลิฟอร์เนีย

นายมนพร เมษาคัม<sup>1</sup>, อาจารย์ ดร. เครือวัลย์ จันทร์แก้ว<sup>1</sup>,

ศาสตราจารย์ J. Michael Moldowan<sup>2</sup> และ David A. Zinniker<sup>2</sup>

<sup>1</sup>ภาควิชาธรณีวิทยา คณะวิทยาศาสตร์ จุฬาลงกรณ์มหาวิทยาลัย

<sup>2</sup>ภาควิชาธรณีวิทยาและวิทยาศาสตร์สิ่งแวดล้อม มหาวิทยาลัยสแตนฟอร์ด

โทรศัพท์: 086-1258439, อีเมล: monpornm@gmail.com

## บทคัดย่อ

การวิจัยในครั้งนี้มุ่งเน้นในการศึกษาเกี่ยวกับไดอะมอนดอยด์และไบโอมาร์กเกอร์ในน้ำมันจากแองซาน ไฮควิน และแองซานต้า บาร์บารา เพื่อพิสูจน์ว่ามีการผสมกันของปิโตรเลียมที่เคลื่อนมาจากหินต้นกำเนิดมากกว่า 1 บริเวณของทั้งสองแอ่งนี้ ซึ่งอาจจะค้นพบการเคลื่อนตัวขึ้นมาจาก cracked oil จากที่ลึก ซึ่งเป็นน้ำมันที่การศึกษาในอดีตอาจจะมองข้ามไป และเป็นแหล่งน้ำมันที่จะมีความสำคัญในอนาคตอันใกล้ที่ความต้องการน้ำมันปิโตรเลียมมีมากขึ้นทุกวัน โดยการวิจัยในครั้งนี้ได้ใช้สารละลายมาตรฐานและเครื่อง Gas Chromatography-Mass Spectrometry (GCMS) ในการระบุชื่อและหาความเข้มข้นของสารประกอบไฮโดรคาร์บอนทั้งสองชนิด (ไดอะมอนดอยด์และไบโอมาร์กเกอร์) จากการวิเคราะห์ไดอะมอนดอยด์ทั้งหมด 89 ตัวอย่างพบว่า 42 (18\*+24\*\*) ตัวอย่างเป็น uncracked oil ที่มีความเข้มข้นของไดอะมอนดอยด์ต่ำ (<2 พีพีเอ็ม), 38(24\*+14\*\*) ตัวอย่างมีการเข้ามาผสมของ cracked oil จากที่ลึกเล็กน้อย ซึ่งมีความเข้มข้นของไดอะมอนดอยด์ 2-10 พีพีเอ็ม และมี 9 (5\*+4\*\*) ตัวอย่างที่มี cracked oil เข้ามาผสมในปริมาณมาก ซึ่งมีความเข้มข้นของไดอะมอนดอยด์มากกว่า 10 พีพีเอ็ม ส่วนการวิเคราะห์ไบโอมาร์กเกอร์นั้นบ่งชี้ว่าหินต้นกำเนิดน้ำมันของแองซาน ไฮควิน และแองซานต้า บาร์บารานี้มีการสะสมตัวในสภาพแวดล้อมแบบไหล่ทวีปและลาดทวีปที่มีความเค็มสูงและประกอบไปด้วยสิ่งมีชีวิตพวกแพลงก์ตอนและสาหร่ายทะเลเป็นหลักตามลำดับ โดยสรุปแล้ว น้ำมันของทั้งสองแอ่งนี้มีระดับ maturity ที่ค่อนข้างสูง, มีระดับการย่อยสลายของปิโตรเลียมโดยจุลินทรีย์ที่หลากหลาย และได้มาจากหินต้นกำเนิดน้ำมันหลายยุคที่ระดับความลึกต่างๆกัน (ครีเทเชียส, พาลีโอจีน และนีโอจีน)

# Contents

	pages
Acknowledgement	a
Abstract in English	b
Abstract in Thai	c
List of Figures	f
List of Tables	h
<b>CHAPTER I INTRODUCTION</b>	<b>1</b>
1.1 Introduction	1
1.2 Problem defined	1
1.3 Hypothesis	2
1.4 Objectives	2
1.5 Scope of work	2
1.6 General statements	2
1.6.1 Petroleum geochemistry	2
1.6.2 Diamondoids	3
1.6.3 Biomarkers	3
1.7 Study areas	4
1.7.1 San Joaquin Basin	4
1.7.2 Santa Barbara Basin	6
1.8 Theory and relevant research	8
1.8.1 Regional geology of Southern California	8
1.8.2 Behavior of diamondoids and biomarkers with maturity	9
1.9 Expected outcomes	10
<b>CHAPTER II METHODOLOGY</b>	<b>11</b>
2.1 Research procedure	11
2.2 Oil samples	12
2.3 Gas Chromatography with a Flame Ionization Detector (GC-FID)	18
2.4 Spiking and Liquid Chromatography (LC)	18

	pages
2.5 Gas Chromatography-Mass Spectrometry (GC-MS)	19
2.6 Compound identification and calculation of diamondoid and biomarker parameters	19
2.7 Data interpretation	20
<b>CHAPTER III RESULT AND INTERPRETATION</b>	<b>21</b>
3.1 Diamondoids	21
3.2 Biomarkers	26
3.2.1 Pristane/phytane ratio	26
3.2.2 Pristane/ <i>n</i> C <sub>17</sub> and Phytane/ <i>n</i> C <sub>18</sub>	26
3.2.3 Ts/(Ts+Tm)	31
3.2.4 Oleananes and oleanane index	33
3.2.5 Homohopane isomerization	37
3.2.6 Gammacerane	38
3.2.7 C <sub>35</sub> homohopane	38
3.2.8 <i>n</i> -alkane distributions	38
3.2.9 C <sub>27</sub> -C <sub>28</sub> -C <sub>29</sub> steranes	40
3.2.10 C <sub>26</sub> -C <sub>27</sub> -C <sub>28</sub> triaromatic steroids	42
<b>CHAPTER IV DISCUSSION, CONCLUSION AND RECOMMENDATION</b>	<b>45</b>
4.1 Discussion	45
4.2 Conclusion	46
4.3 Recommendation	48
<b>REFERENCES</b>	<b>49</b>
<b>APPENDIX</b>	<b>52</b>
Appendix I Biodegradation ranking	53
Appendix II Tectonic evolution of the San Joaquin Basin	54

## List of Figures

		pages
Figure 1.1	The relation between lattice diamond structure and (i) adamantane, (ii) diamantane and (iii) triamantane structures (Mansoori, 2007).	3
Figure 1.2	Molecular structure of oleanane which is transformed from taraxer-14-ene and olean-12-ene which is generated from flowering plants (Moldowan <i>et al.</i> , 1994).	4
Figure 1.3	Map of the San Joaquin Basin (gray shading) (Modified from Lillis and Magoon, 2004).	5
Figure 1.4	North-south chronostratigraphic correlation chart of the San Joaquin Basin (Johnson and Graham, 2007).	5
Figure 1.5	Map of the Santa Barbara Basin (green shading) (Modified from Galloway, 2009).	6
Figure 1.6	Santa Barbara Basin stratigraphic sequences (Galloway, 2009).	7
Figure 1.7	San Andreas Fault zone with California map (Tasa Graphic Arts, Inc., 2009).	9
Figure 1.8	The correlation between the diamondoid concentrations (methyl-diamantanes) and biomarker concentration (C <sub>29</sub> $\alpha\alpha\alpha$ stigmastane 20R) in oils of different thermal maturities, cracked and uncracked (Dahl <i>et al.</i> , 1999).	10
Figure 2.1	Methodology flow chart.	11
Figure 3.1	The relationship between 3- + 4- methyl diamantanes and C <sub>29</sub> $\alpha\alpha\alpha$ stigmastane 20R in oil from the San Joaquin and Santa Barbara Basins showing the diamondoid baseline	21
Figure 3.2	A Crossplot of pristane/nC <sub>17</sub> versus phytane/nC <sub>18</sub> , plot modified from Shanmugam (1985)	27
Figure 3.3	A Crossplot of Ts/Tm versus Ts/(Ts+Tm)	32
Figure 3.4	A crossplot of C <sub>31</sub> [22S/(22S+22R)] versus C <sub>32</sub> [22S/(22S+22R)]	37
Figure 3.5	n-alkane distributions of non-biodegraded oil samples from the San Joaquin Basin	39

		pages
Figure 3.6	<i>n</i> -alkane distributions of non-biodegraded oil samples from the Santa Barbara Basin	40
Figure 3.7	C <sub>27</sub> -C <sub>28</sub> -C <sub>29</sub> steranes ternary diagrams of oils from the San Joaquin Basin	41
Figure 3.8	C <sub>27</sub> -C <sub>28</sub> -C <sub>29</sub> steranes ternary diagrams of oils from the Santa Barbara Basin	42
Figure 3.9	C <sub>26</sub> -C <sub>27</sub> -C <sub>28</sub> triaromatic steroids ternary diagrams of oils from the San Joaquin Basin	43
Figure 3.10	C <sub>26</sub> -C <sub>27</sub> -C <sub>28</sub> triaromatic steroids ternary diagrams of oils from the Santa Barbara Basin	44
Figure 4.1	Pie charts showing the types of oil of the San Joaquin and Santa Barbara Basins	46
Figure 4.2	Biomarker parameters respond in different maturity levels. Parameters shown include Ts/(Ts+Tm) ratio and homohopane isomerization ratios used in this research (Peters <i>et al.</i> , 2005).	47
Figure 4.3	Pie charts showing proportions of oils with different biodegradation ranks (based on Peters and Moldowan, 1993) of oil samples from the San Joaquin and Santa Barbara Basins.	48
Figure A-1	Tectonic evolution of the San Joaquin Basin. Topography- and compaction-driven flow are shown as arrows. The active tectonics include uplift of the Sierra Nevada beginning 5–10 Ma, the rise of the Coast Ranges above sea level (S.L.) and the last marine regression starting on 2 Ma. Dashed, gray, dark stippled, light stippled, and hachured units represent Post-Pliocene, Pliocene, Miocene, Pre-Miocene, and Sierran rocks, respectively (Wilson <i>et al.</i> , 1999).	54



## List of Tables

		pages
<b>Tables 2.1</b>	Oil samples from the San Joaquin (gray boxes) and Santa Barbara (blue boxes) Basins with their details and weights	13
<b>Tables 3.1</b>	Concentrations of adamantane, 3- + 4- methyl diamantanes and C <sub>29</sub> $\alpha\alpha\alpha$ stigmastane 20R in oil from the San Joaquin (gray boxes) and Santa Barbara (blue boxes) Basins	22
<b>Tables 3.2</b>	The ratios of Pr/Ph, Pr/nC17, Ph/nC18, Ts/Tm and Ts/(Ts+Tm) with biodegradation ranks (based on Peters and Moldowan, 1993) of the oil samples from the San Joaquin (gray boxes) and Santa Barbara (blue boxes) Basins	28
<b>Tables 3.3</b>	Oleanane index, homohopane isomerization ratios, gammacerane and C <sub>35</sub> homohopane of the oil samples from the San Joaquin (gray boxes) and Santa Barbara (blue boxes) Basins	33
<b>Table 4.1</b>	Intensely cracked oils' platform of the San Joaquin and Santa Barbara Basins	46
<b>Table A-1</b>	Biodegradation ranking based on Peters and Moldowan (1993), double arrow means disappear	53

# CHAPTER I

## INTRODUCTION

### 1.1 Introduction

Petroleum exploration heavily relies on result from geophysical survey (i.e. seismic survey) to characterize sedimentary architectures, faults, folds and traps for predicting an area which may have potential to be petroleum reservoir. Moreover, the exploration also utilized petroleum geochemistry, such as biomarker analysis, to anticipate the potential of source rock to generate petroleum. Both geophysics and biomarkers can only be used reasonably effectively in shallow petroleum exploration. Geophysical data from deep areas provide a challenge in interpretation. Biomarkers are not stable at high temperatures (direct variation with depth), so they are all annihilated.

Nowadays, demand for petroleum is continually increasing, so we have to explore for more petroleum in new areas and at greater depths in existing producing areas. In the last ten years, geochemists developed a new technique for petroleum exploration in deep areas. It is diamondoid analysis. Diamondoids are highly stable at high temperatures, so they do not vanish at greater depths. We can use the diamondoid analysis to predict if we have other deep reservoirs which can be new prospects of petroleum exploration for our time. When we combine the diamondoid analysis and geophysical survey together, we probably can anticipate more new potential reservoirs precisely.

### 1.2 Problem defined

American geologists have not studied the diamondoids in San Joaquin and Santa Barbara Basins before, so no one knows where the oil fields that contain inputs from cracked sources are. In addition, United States Geological Survey (USGS), California Office desire to study more petroleum systems in these two basins. This senior project was inspired by these two reasons, to prove if these two basins contain any deep cracked source or not.

### 1.3 Hypothesis

1. Most oil samples from the San Joaquin and Santa Barbara Basins are uncracked oils with low diamondoid concentrations, but some samples may have inputs from deep cracked sources so they contain relatively higher diamondoid concentrations.

2. The San Joaquin and Santa Barbara Basins are different in depositional environments, so their biomarker distributions should differ from each other.

### 1.4 Objectives

1. To identify mixed petroleum sources in these well-explored basins allowing for the discovery of possible previously unrecognized cracked oil inputs from deeper sources.

2. To compare the biomarker distributions in oil samples from the San Joaquin and Santa Barbara Basins by using geochemical techniques.

### 1.5 Scope of work

This research project focuses on analyzing 47 and 42 oil samples from the San Joaquin and Santa Barbara Basins to specify the oil fields that contain inputs from deep cracked sources, as indicated by high diamondoid concentrations and to reveal the types of oil, maturity levels, depositional environment, source inputs, and biodegradation.

### 1.6 General statements

#### 1.6.1 **Petroleum geochemistry**

Petroleum geochemistry is an important technique in the exploration and production of petroleum. It is a discipline that includes the applications of organic geochemistry to study origin, formation, migration, accumulation and alteration of petroleum (Magoon and Dow, 1994).

In particular, petroleum geochemistry is a tool that can improve exploration efficiency by identifying the processes that lead to the availability of petroleum in reservoirs. These processes include the input, accumulation and preservation of organic matter in depositional environments, its burial history in the sediment, and its alteration.

Applications of petroleum geochemistry can be summarized into 4 main schemes: (1) petroleum systems (2) biomarkers and stable isotopes for oil-oil and oil-source rock correlations (3) 3-D basin modeling and (4) secondary processes such as biodegradation, water-washing and migration that alter the composition and usually degrade the quality of petroleum (Peters and Fowler, 2002).

### 1.6.2 Diamondoids

Diamondoids are ultra-stable, saturated hydrocarbons. They have a diamond-like structure consisting of six-member carbon rings fused together. They are called "diamondoids" because their carbon-carbon framework constitutes the fundamental repeating unit in the diamond lattice structure as shown in Figure 1.1. The fundamental formula of diamondoid can be concluded in  $C_{4n+6}H_{4n+12}$ , which n starts from one. Adamantane is the smallest diamondoid which consists of one sub-unit of diamond lattice structure (Mansoori, 2007).

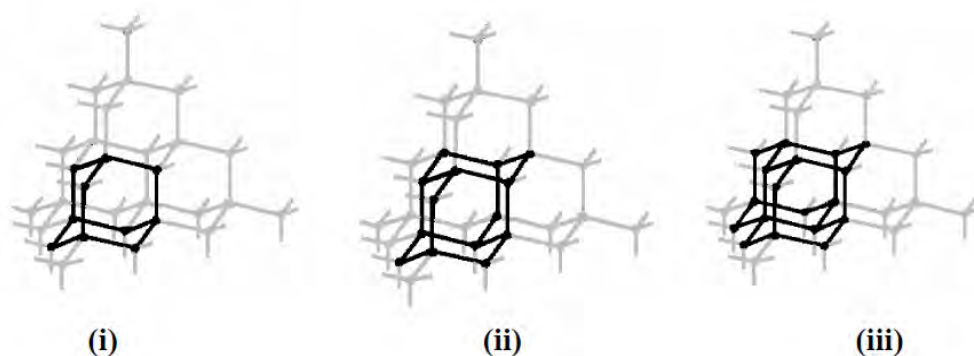


Figure 1.1: The relation between lattice diamond structure and (i) adamantane, (ii) diamantane and (iii) triamantane structures (Mansoori, 2007).

### 1.6.3 Biomarkers

Biomarkers are compounds that organisms produced, and then they were transformed during diagenesis-catagenesis to form another compound that had a similar molecular structure to the precursor and are collected in oil. Figure 1.2 shows an example of biomarker and its precursor.

Biomarkers are important hydrocarbon compounds which can be used to make oil-oil and oil-source rock correlations. The biomarker distributions in oil can be used to infer characteristics of the source rock that generated the oil without examining the source rock from core drilling itself. Moreover, biomarkers can reveal the kerogen type, the age of the source rock, the depositional environment such as marine, lacustrine, delta or hypersaline, the lithology of the source rock

(carbonate and shale) and the thermal maturity of the source rock during generation (Peters and Moldowan, 1993).

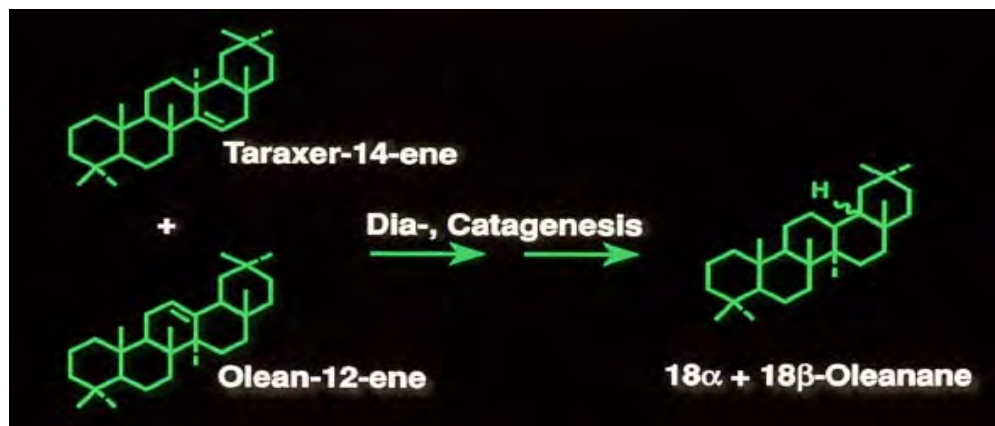


Figure 1.2: Molecular structure of oleanane which is transformed from taraxer-14-ene and olean-12-ene which is generated from flowering plants (Moldowan *et al.*, 1994).

## 1.7 Study areas

### 1.7.1 San Joaquin Basin

The San Joaquin Basin (Figure 1.3) is a major petroleum province located in the southern half of California's Great Valley. It is approximately 700 km long. It is an asymmetrical basin that originated between a subduction zone to the west and the Sierra Nevada to the east. Sedimentary fill-up and tectonic structures in the San Joaquin Basin have been recorded from Mesozoic through Cenozoic. Sedimentary architecture in the San Joaquin Basin is complicated because of its tectonic regimes, its lateral changes in depositional environment and temporal changes in relative sea level. The basin is filled with marine sediments overlain by continental sediments. There are some places deposited largely by streams draining mostly from the mountains, and partially by lakes that inundated portions of the basin from time to time. Most of the continental sediments are fine-grained: clay, sandy clay, sandy silt, and silt.

The San Joaquin Basin is filled with organic-rich marine rocks of Late Cretaceous, Eocene, and Miocene ages providing the source of most of the oil and gas during periods of sea level transgression and anoxia (Figure 1.4). Generated on the basin's west side, hydrocarbons migrated into nearly every facies type in the basin; from shelf and submarine fan sands, diatomite, shale, nonmarine coarse-grained rocks and schist (Scheirer and Magoon, 2007).

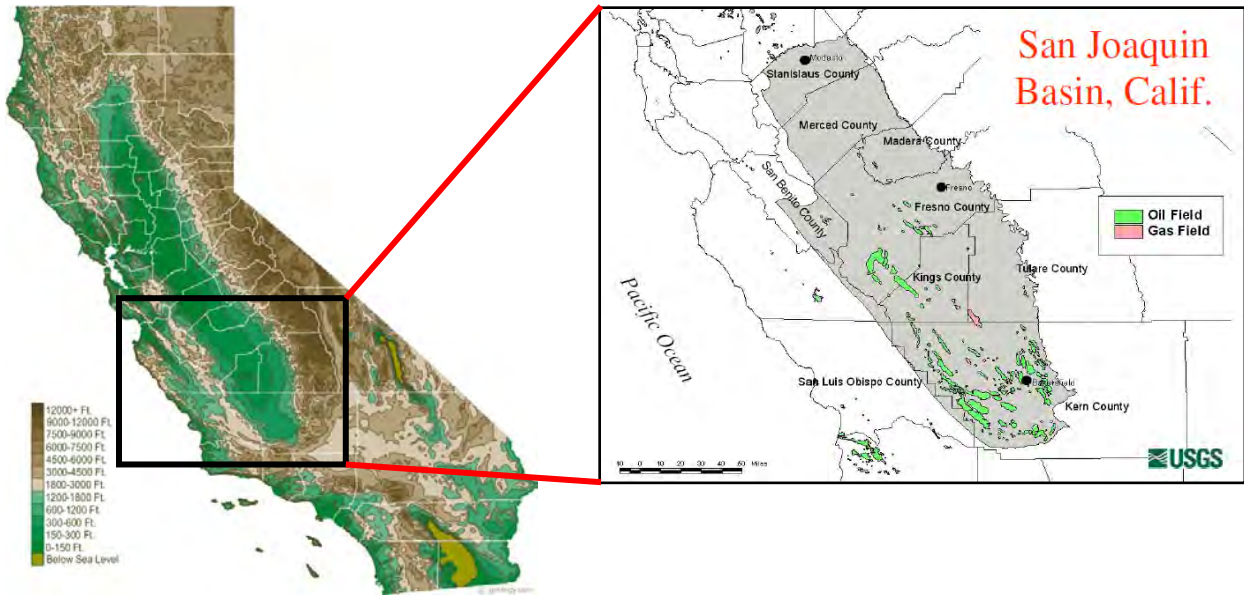


Figure 1.3: Map of the San Joaquin Basin (gray shading) (Modified from Lillis and Magoon, 2004).

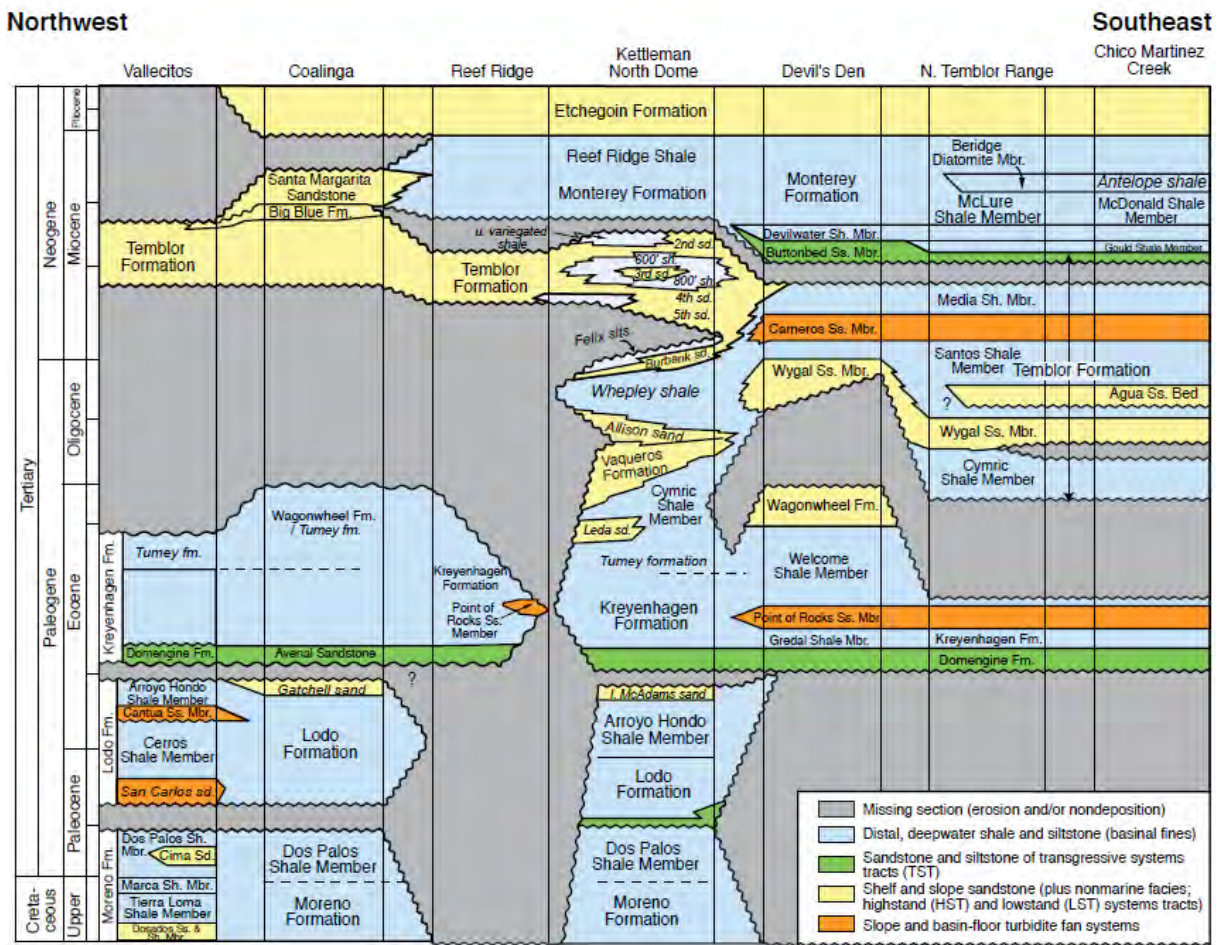


Figure 1.4: North-south chronostratigraphic correlation chart of the San Joaquin Basin

(Johnson and Graham, 2007).

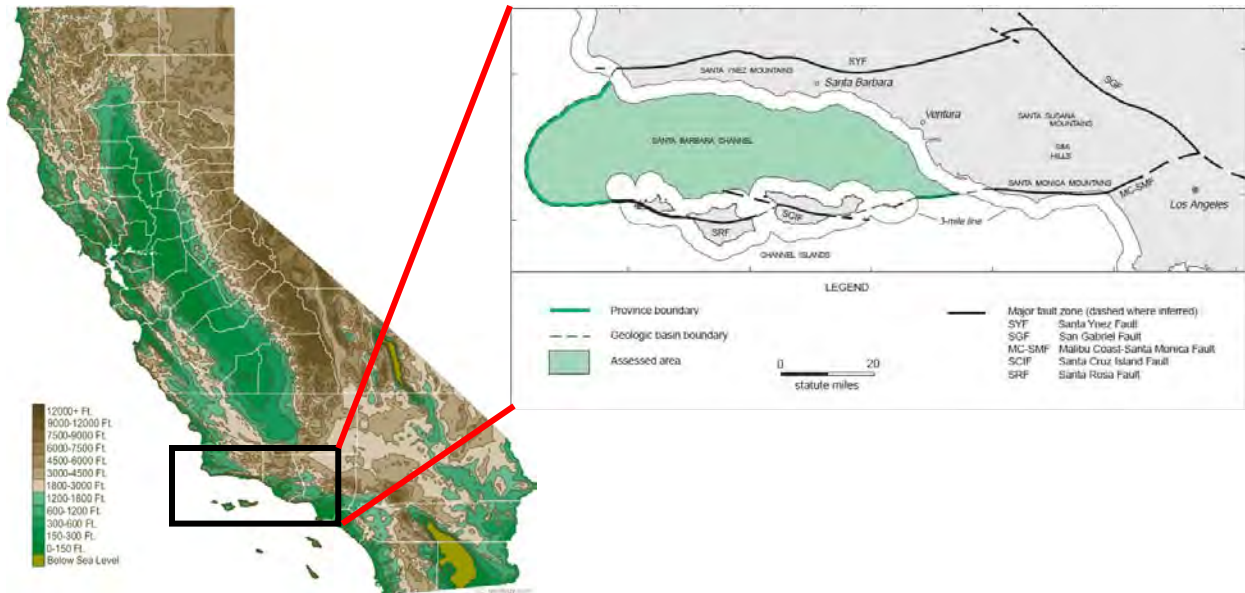


### 1.7.2 Santa Barbara Basin

The Santa Barbara Basin is located in Southern California's offshore (Figure 1.5). This offshore basin is within the western portion of the Transverse Ranges geomorphic province which is named because its east-west orientation runs counter to the predominant north-northwest orientation of the region's major structural trends.

The oldest known sedimentary rocks in the basin were dated from the Early Cretaceous (Figure 1.6). The sediments are deposited on a probable metamorphic/meta-sedimentary basement complex. Mesozoic- and Paleogene-aged rocks in the modern Santa Barbara Basin were originally deposited in a forearc setting. This sequence of Cretaceous to lower Oligocene is predominantly marine sedimentary rock.

There are five source rocks (Cretaceous, Eocene, Oligocene, Miocene and Pliocene) in the basin. Oil and gas that are generated will migrate to nearly every formation (Cretaceous through Pleistocene). The most important reservoirs are sandstones and fractured biogenic siliceous shales (Galloway, 2009).



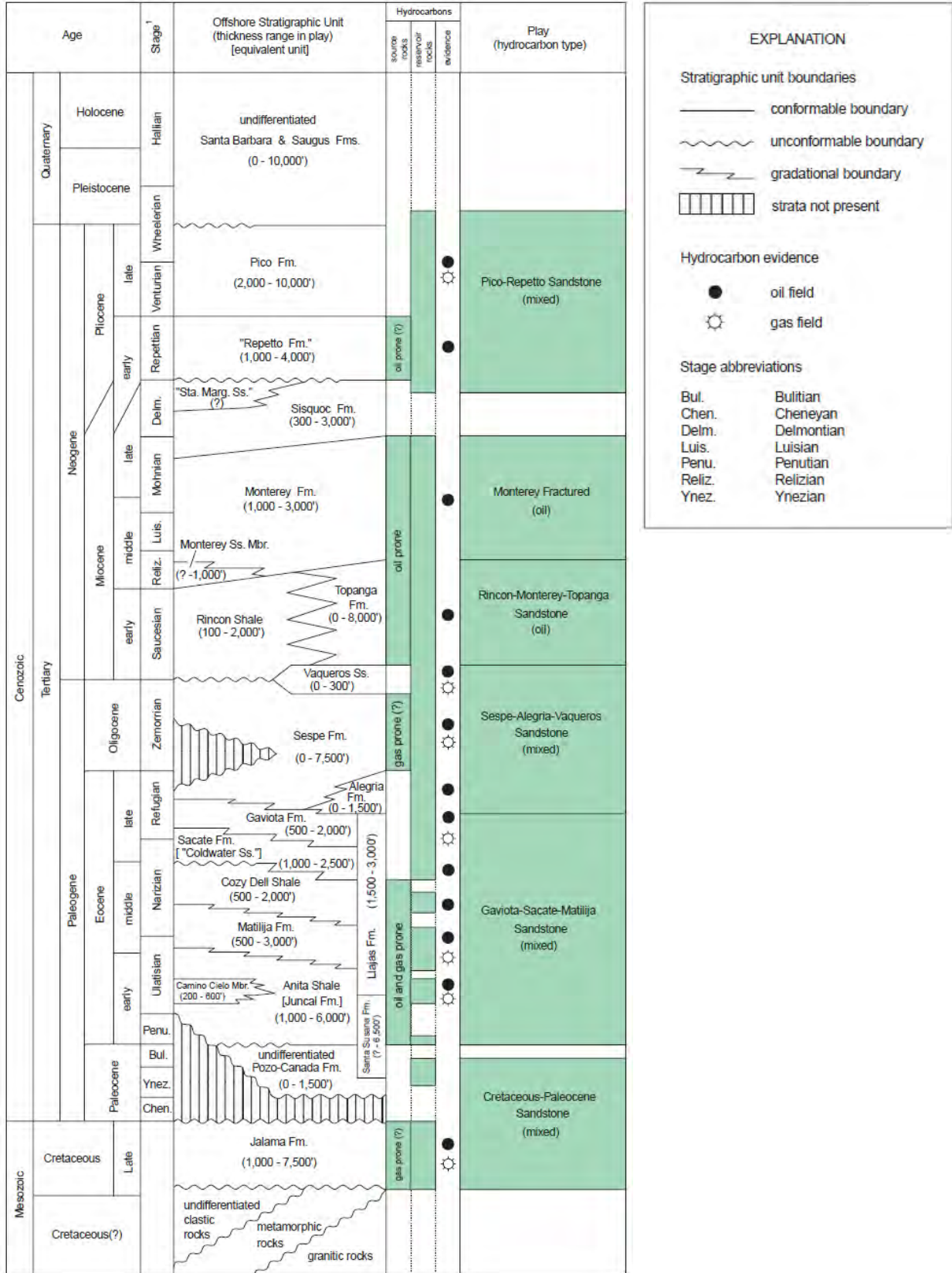


Figure 1.6: Santa Barbara Basin stratigraphic sequences (Galloway, 2009).



## 1.8 Theory and relevant research

### 1.8.1 Regional geology of Southern California

The unique landscape of Southern California is extremely varied, with high mountains, expansive deserts, sandy and rocky beaches, bushy hills, and broad river valleys in close proximity to each other.

Eight physiographic provinces are represented in the varied terrain of Southern California: the Southern Sierra Nevada, the Southern Coast Ranges, the Southern Great Valley, the Transverse Ranges, the Peninsular Ranges, the Colorado Desert, the Mojave Desert, and the main part of the Basin and Range.

The rocks of Southern California are extremely varied. Igneous rocks are exposed in many places. Mesozoic plutonic rocks similar to granite and Cenozoic volcanic rocks are basalt, rhyolite and tuff. Sedimentary rocks are also widespread including Mesozoic and Cenozoic shale and sandstone of marine origin along with thick sequences of Cenozoic terrestrial sedimentary rocks. Metamorphic rocks are not common. They are represented primarily by schist and gneiss of either Pre-Cambrian or Mesozoic age.

The mountains of Southern California are relatively young and have formed through normal faulting under tension in the Basin and Range, folding and reverse faulting generated by compression in the Transverse Range, and through oblique faulting related to shear stress in several places along the San Andreas Fault zone as shown in Figure 1.7.

Over the past 800 million years, the western edge of the North American continent has been affected by several different plate tectonic interactions and events, including continental rifting, a passive continental margin, a continental-oceanic convergent plate boundary, and a transform plate boundary. Each of these plate tectonic settings affected the bedrock foundation of Southern California (DeCourten, 2006).



Map showing only a few of the many splinter faults that are part of this great fault system.

Figure 1.7: San Andreas Fault zone with California map (Tasa Graphic Arts, Inc., 2009).

### 1.8.2 Behavior of diamondoids and biomarkers with maturity

Diamondoids are mainly used to identify the occurrence and estimate the extent of oil annihilation and the oil deadline (temperature and depth that ultimately converts oil into gas and pyrobitumen) in a particular basin. They also can be used to identify oils consisting of mixtures of high- and low-maturity components. Methyl-diamantanes are used for x-axis (Figure 1.8) because they have relatively high concentrations and are the smallest diamondoids which are not readily lost to evaporation. Furthermore, adamantane which has the highest diamondoid concentration can be biodegraded a little bit (Grice, *et al.*, 2000), so methyl-diamantanes are suitable choices to use to

correlate with biomarkers. C<sub>29</sub>  $\alpha\alpha\alpha$  stigmastane 20R was chosen for y-axis because it is a commonly found biomarker in oils and it disappears at the time which diamondoid concentrations begin to rise. The shape of the curve is the result of decreasing biomarker concentration with increasing thermal maturity (moving down the y-axis), followed by the oil cracking, resulting in increased diamondoid concentrations due to their high thermal stability (Dahl, *et al.* 1999).

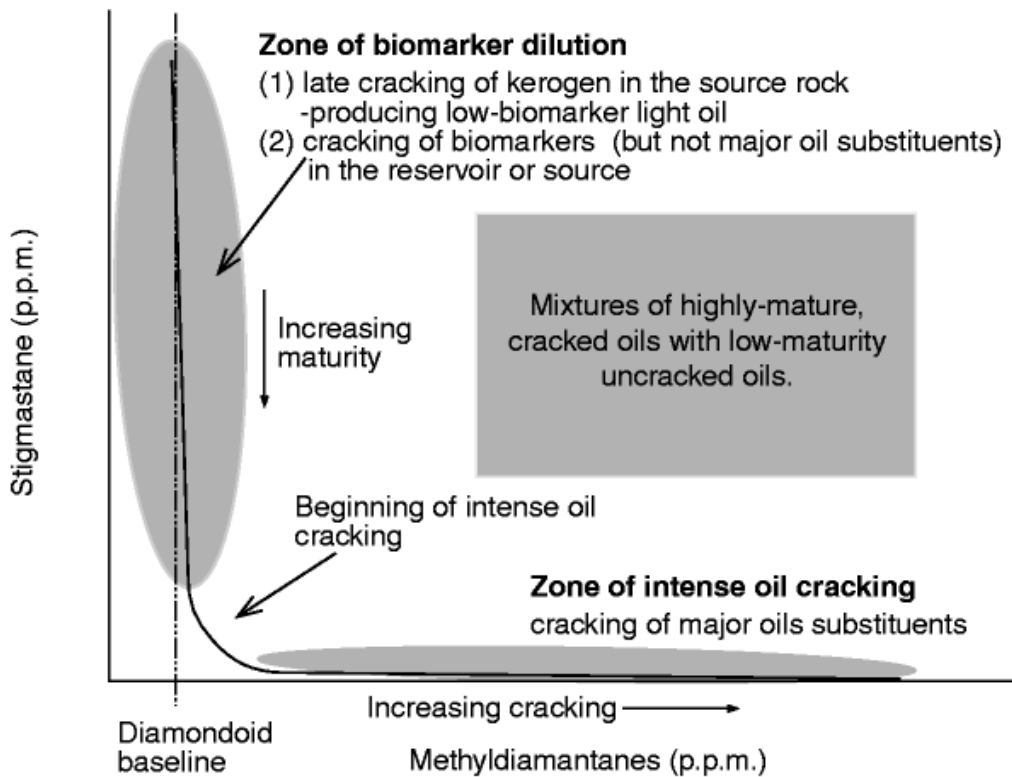


Figure 1.8: The correlation between the diamondoid concentrations (methyl-diamantanes) and biomarker concentration (C<sub>29</sub>  $\alpha\alpha\alpha$  stigmastane 20R) in oils of different thermal maturities, cracked and uncracked (Dahl *et al.*, 1999).

### 1.9 Expected outcomes

1. Specify the oil fields that contain inputs from deep cracked sources generating high diamondoid concentrations.
2. Explain petroleum systems in the San Joaquin and Santa Barbara Basins in more detail by using biomarker distributions.

## CHAPTER II METHODOLOGY

### 2.1 Research procedure

The method of investigation used in this project is summarized as a flow chart in Figure 2.1.

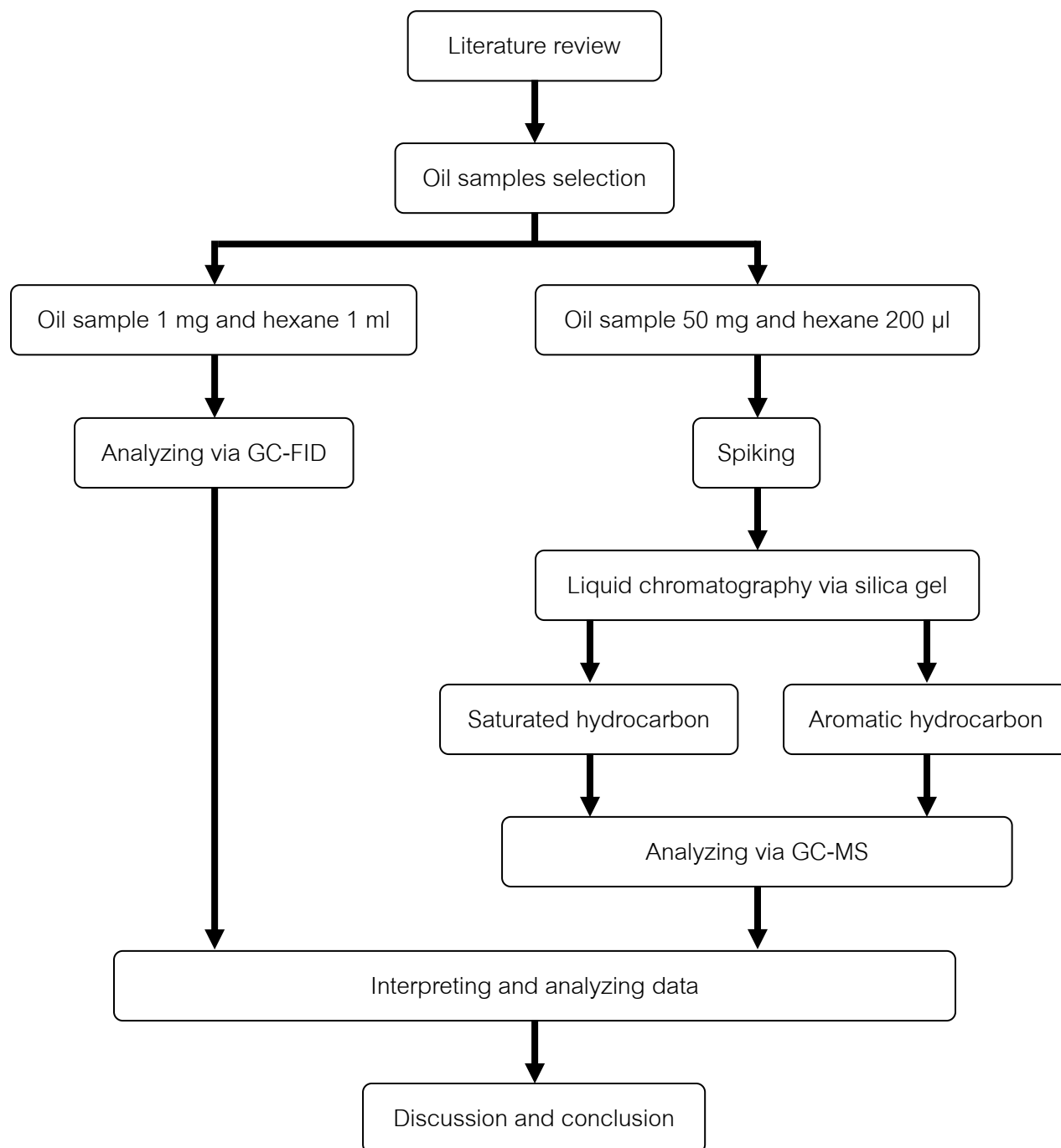


Figure 2.1: Methodology flow chart.

The first step of the research concerns literature reviews on regional geology of Southern California, the San Joaquin and Santa Barbara Basins, basic concepts of organic geochemistry, petroleum geochemistry, diamondoids and biomarkers.

The second step is oil sample selection (Table 2.1). The oil samples were collected by various oil companies from different platforms in the San Joaquin and Santa Barbara Basins. Eighty nine oil samples were selected for this study. This step also includes oil sample weighing.

The third step is quantifying amount of *n*-alkanes and isoprenoids in each oil sample by using Gas Chromatography with a Flame Ionization Detector (GC-FID).

The fourth step is separating saturated and aromatic hydrocarbons in each oil sample by using Liquid Chromatography (LC) technique. Both saturated and aromatic hydrocarbon fractions were analyzed via Gas Chromatography-Mass Spectrometry (GC-MS). Moreover, diamondoids and biomarkers identification is included in this step.

The final step is discussion and conclusion of the data in terms of cracked oil platforms, types of oil, maturity levels, depositional environment, source inputs, and biodegradation.

## **2.2 Oil samples**

Oil samples from various platforms of the San Joaquin and Santa Barbara Basins were provided by Department of Geological and Environmental Science, Stanford University and United States Geological Survey (USGS), California Office. About 50 mg of each sample was collected to study diamondoids and biomarkers, but the weights were collected depending on the amount of the available samples which range from 2-110 mg (Table 2.1).

Samples	Details	Weight (mg)
MP-001	GCMS 258-1, CFRC 35533, Mckittrick Field, Well 511-17Z, Kern Co. California, Caneros Formation	54.50
MP-002	GCMS 36, CRC 31394, San Joaquin Valley	56.27
MP-003	CRC 29839, Baldwin 77, Montebello Field, Pliocene, Whole crude, Sampled 10/23/75	73.86
MP-004	GCMS 258, CRC 30931-2, Mckittrick Field, Well 511-17Z, Kern Co. California, Caneros Formation, Miocene	48.56
MP-005	J.H. Elison Ashurst, Sample VS-4, Sampled 10/21/85	60.59
MP-006	Tannehill Oil Co. F&I Well, Sample VS-6, Sampled 10/21/86	49.86
MP-007	Oil City Field, Fresno, Coast Range Oil Co. Moreno Formation, Cretaceous, Sampled 12/15/86	65.21
MP-008	Silver Creek Field, Vallecitos, Sampled 2/11/11	38.84
MP-009	J.H. Elison Ashurst 2-27	45.50
MP-010	J.H. Elison Ashurst 52A-33	65.39
MP-011	F&I Seep 2, Canyon, Sampled 2/11/11	109.31
MP-012	F&I Section 29, Sampled 2/11/11	55.84
MP-013	Panoche Vallecitos Oil	56.75
MP-014	F&I 26-31, Sampled 2/11/11	62.55
MP-015	F&I 16-31, Sampled 2/11/11	79.78
MP-016	GCMS C254, Jacobson 572-182, Mckittrick Field, Sampled 12/10/98	52.21
MP-017	CRC 26833, Project 64626, SOCal 588-150, Mckittrick Field, Caneros Formation	56.80
MP-018	Midway Sunset Crude	41.33

Table 2.1: Oil samples from the San Joaquin (gray boxes) and Santa Barbara (blue boxes) Basins with their details and weights.

Samples	Details	Weight (mg)
MP-019	CRC 18457, Project 32293, SOCal Mcphee 36W, Cymric Field, Amnicola Formation, Pleistocene	96.34
MP-020	GCMS 214, CRC 35203, SOCal 2-4, Cymric Field, San Joaquin Valley, Amnicola Formation, Biodegradation	96.87
MP-021	GCMS 62, CRC 23137, Buena Vista Hills Field, San Joaquin Valley, Sand Formation, Pliocene	43.38
MP-022	GCMS 61, CRC 23022, Mckittrick Field, Pliocene	60.16
MP-023	GCMS 985, CRC 34709-2, Monterey Field, PT. Arguello Oil, California	67.70
MP-024	GCMS 60, CRC 32515, San Joaquin Valley, Kern River	89.86
MP-025	Tarwater Creek Field, Pescadero Co.	65.53
MP-026	GCMS 37, CRC 31394-1, Buena Vista Hills Field, Kern Co. California, Antelope Shale Formation, Pliocene	65.41
MP-027	GCMS 58, CRC 32514, SOCal Tee 2-7, Poso Creek Field, San Joaquin Valley, Chanac Formation, Pliocene	45.87
MP-028	GCMS 275, CRC 32511, Project 4070, Race Track Field, Lower Miocene, Biodegradation	58.92
MP-029	GCMS 980, Four Deer Field, Los Flores Ranch Well, Arguello Oil Co. California	46.11
MP-030	GCMS 754, CRC 41635-1, Monterey, California	79.87
MP-031	Mckittirck Oil Seep, Sampled 6/22/11, 35 17' 35.5" North, 117 38' 7.4" West	32.98
MP-032	GCMS 277, CRC 36241, Biodegradation Oil, Sampled 2/6/78	63.21
MP-033	GCMS 259, CRC 23616, Mckittrick, No more in LA Habra 2nd Caverns, Whole Crude Box 16, Sampled 4/26/84	47.04
MP-034	GCMS 11, CRC 24206, Railroad Gap Field, Kern Co., Antelope Shale Formation, Upper Miocene	59.00
MP-035	Kettleman Field, Kettleman City, Well No. 4-9	67.23
MP-036	Catalog 97-56, Old Joel Flat, Petrolia Hidden Valley, Oil	67.81

Table 2.1 (continued): Oil samples from the San Joaquin (gray boxes) and Santa Barbara (blue boxes) Basins with their details and weights.

Samples	Details	Weight (mg)
MP-037	Macon 36126, Elk Hills Oil Field, Uonpra No. 1371-17R, Sampled 8/3/98	56.56
MP-038	Macon 29085, Coalinga Oil Field, Depth 1193', Sampled 8/3/98	20.93
MP-039	Macon 50263, Jacalitos Oil Field, Sampled 8/3/98	77.50
MP-040	Macon, San Ardo Field, Anrignac, Sampled 8/3/98	75.59
MP-041	Macon/Cal 0283\$, Oil Creek Field, Costa No. 7-A, Sampled 8/3/98	34.50
MP-042	Macon 46539, Sargent Oil Field, Sargent 10, Sampled 8/3/98	31.76
MP-043	GCMS 7, CRC 23117-1, Chevron 19 Pair, Well 555-15Z, Antelope Shale Oil Field, Sampled 9/17/76	37.52
MP-044	Midway Sunset 31E, ASL0001, Well 5-3A, Pliocene, Sampled 5/5/81	68.79
MP-045	GCMS 5, CRC 13896-2, Well Kreyenhagen, Depth 10967-10973', Sampled 8/26/74	32.49
MP-046	GCMS 3, CRC 13832, SOCal 38, Kern Co. California, Kreyenhagen Formation, Eocene	79.08
MP-047	GCMS 2, CRC 13833, Stock Tank Oil, Kern Co. California, N. Leda Pool, Leda Formation, Miocene	52.49
MP-048	Catalog 09-105, Gaviota I, Solitary Tarmound, Seep Tar	26.58
MP-049	Catalog 99-109, La Honda D.F. South 16, Oil	74.28
MP-050	Catalog 02-86, Platform Holly, 3120-11, Depth 7447', Oil	37.00
MP-051	Catalog 02-85, Platform Holly, 3120-8, Depth 4989', Oil	12.82
MP-052	Catalog 02-66, Gaviota Offshore, Oil Seep, Tar	33.99
MP-053	Catalog 08-156, Hamp Lease Seep, Ojai Silverthread, Oil Seep	24.24
MP-054	Catalog 04-322, Summerland Offshore, Oil Seep	16.98

Table 2.1 (continued): Oil samples from the San Joaquin (gray boxes) and Santa Barbara (blue boxes) Basins with their details and weights.



Samples	Details	Weight (mg)
MP-055	Catalog 10-160, Cojo 2 Sample Tar Vents, Seep Tar	28.51
MP-056	Catalog 09-112, Cojo 1 Tarmound, Seep Tar	12.86
MP-057	Catalog 08-191, Platform Heritage, Produced Oil	46.88
MP-058	Catalog 08-178, Platform B Well B-34, Produced Oil	54.22
MP-059	Catalog 05-9, Platform Heritage, Produced Oil	55.90
MP-060	Catalog 08-170, Platform Henry, Well 16-B, Produced Oil	29.76
MP-061	Macon 31908-1, Belridge North, Pliocene, Sampled 8/3/98	35.66
MP-062	Aera 15, OCS-P-416-1, DST 8A, Sampled 3/28/84, Resampled 6/21/11	26.01
MP-063	Aera 14, OCS-P-0416-1, DST 6, Sampled 6/19/84, Resampled 6/21/11	86.72
MP-064	05-348, Summerland, Becker Onshore Well, Seep	77.39
MP-065	T526-G72, Guyamas Seep	64.94
MP-066	Aera 1, OCS-P-0231 # 5, DST 1	47.43
MP-067	Platform B, Well B-9	52.44
MP-068	Platform C, Well C-16	68.66
MP-069	Platform C, Well C-55	25.25
MP-070	Platform C, Well C-59	68.19
MP-071	T526-PC4-1, Guyamas Seep, CB-03-63	62.15
MP-072	35-T27S-R20E, North Belridge Aera Energy, 403030088, 551P3-35N, KB 666, Depth 520-1350'	51.36

Table 2.1 (continued): Oil samples from the San Joaquin (gray boxes) and Santa Barbara (blue boxes) Basins with their details and weights.

Samples	Details	Weight (mg)
MP-073	36-T27S-R20E, North Belridge Aera Energy, 403031096, 22L-36N, KB 623, Depth 536-787', Sampled 6/22/11	51.96
MP-074	36-T27S-R20E, North Belridge Aera Energy, 403041977, 557N3-36N, KB 635, Depth 780-1490'	42.99
MP-075	T197-R8, Escanaba Trough Asphalt	47.60
MP-076	Catalog 97-15, Elwood Field	10.11
MP-077	T522-G13, Guyamas Seep	35.32
MP-078	Platform B, Well B-26	2.00
MP-079	Platform B, Well B-60	12.94
MP-080	Catalog 02-172, Shane Seep, Vent 1, Sample 1, 34 24.370' North, 119 53.408' West, Sampled 09/25/02	80.72
MP-081	Catalog 04-270, Tonya Residue	29.74
MP-082	Catalog 02-173, Shane Seep, Vent 1, Sample 2, 34 24.370' North, 119 53.408' West, Sampled 09/25/02	13.81
MP-083	Catalog 08-232, COP Tarmound Lone, Sample 2, 34.39255 North, 119.8474 West	37.63
MP-084	Catalog 05-6, Platform Hondo, Well H-23, Sampled 2/4/05	53.65
MP-085	Catalog 05-1, Platform Harmony, Well HA-4, Sampled 2/4/05	49.80
MP-086	Catalog 05-5, Platform Hondo, Well H-15, Sampled 2/4/05	70.41
MP-087	Catalog 05-4, Platform Hondo, Well H-3, Sampled 2/4/05	47.67
MP-088	Catalog 05-2, Platform Harmony, Well HA-7, Sampled 2/4/05	58.35
MP-089	Catalog 05-345, La Galeta Seep Sediment, Sampled 9/15/05	43.08

Table 2.1 (continued): Oil samples from the San Joaquin (gray boxes) and Santa Barbara (blue boxes) Basins with their details and weights.

### 2.3 Gas Chromatography with a Flame Ionization Detector (GC-FID)

Each oil sample was prepared from 1 mg of oil sample mixed with 1 ml of hexane in a 1.5 ml vial with tightly fitting cap. GC-FID analysis for all the samples were performed using a Hewlett Packard 5890 GC equipped with a 100% methyl silicone DB-1 capillary column (24 m × 0.2 mm i.d. with film thickness 0.33 μm). Hydrogen served as a carrier gas at a fixed 20 psi head pressure. The oil samples were injected at 80°C and the oven was programmed at 10°C/minute to 320° C where it was held for 15 minute.

### 2.4 Spiking and Liquid Chromatography (LC)

Saturated and aromatic hydrocarbons were separated from the oil samples by using Liquid Chromatography (LC) technique. Two stages of LC were performed by using two solvents. The first stage separates saturated hydrocarbons from the oil samples. Each sample was prepared from a known weight (about 50 mg) of oil sample and about 200 μl of hexane in a 4 ml vial then securely affixes the cap. Samples were spiked with standard solutions (D3 1-methyl-adamantane, D4 adamantane, D3 1-methyl-diamantane, D5 ethyl-diamantane, D4 diamantane, cholane and D4 triamantane; D means deuterium). Next, plugging the tapered end of the glass column with filter paper to retain the silica gel, but allow the solvents to pass through. Filling the column with activated silica gel to a level of 10 cm from the bottom by adding a few cm at a time and tapping or vibrating the column to pack the silica gel tightly and uniformly. Place the packed column in a clamp or rack to hold it vertical. Mark a known weight 1.5 ml vial at the 1 ml level and place it under the column. After that, accurately weighing 10-25 mg of crude oil sample and place it on the top of the column and adding hexane to the top of the column to chromatograph the sample. Continue adding hexane and eluting by gravity, until 1 ml of elute has been collected and tightly affix the cap. Do not allow the level of solvent to drop below the top of the silica gel bed. Control the addition of hexane so that the level of liquid on the column drops just to the top of the silica gel bed when 1 ml has been collected.

In the second stage, the eluting solvent was changed to dichloromethane to separate aromatic hydrocarbons from the remainder. Then, rinse the outside tips of the column into the hexane collection vial with a few drops of hexane, and wipe it with a tissue. Next, mark a known

weight 4 ml vial at the 2 ml level and place it under the column. Continue adding dichloromethane to the top of the column and continue elution until at least 2 ml of eluate has been collected. After that, use gentle pressure to assist the elution. Lastly, rinse and wipe the outside tip of the column as before and evaporate the solvents in the vials with gentle nitrogen stream at 40-50°C. Adding hexane to each vial to transfer solution into a 1.5 ml vial and securely affix the cap.

## **2.5 Gas Chromatography-Mass Spectrometry (GC-MS)**

GC-MS analysis was performed on both saturated and aromatic hydrocarbon fractions by using a Hewlett-Packard 5890 Series II Gas Chromatograph interfaced to a Fisons Instruments Autospec-Q Hybrid Mass Spectrometer. The GC was equipped with a 60 m J&W fused silica DB-1 capillary column (0.25 mm i.d. with 0.25 µm phase thickness of 100% methyl silicone). Hydrogen was used as carrier gas at a constant pressure of 15 psi. The temperature program was set 50°C for 2 minutes, 50-80°C at 15°C/minute, 80-290°C at 2.5°C/minute, 290-320°C at 25°C/minute and 320°C for 25 minutes. The injection port and transfer line temperature was 325°C.

The following ions were monitored for saturated hydrocarbons (including diamondoids) analysis:  $m/z$  135, 136, 140, 149, 177, 187, 188, 191, 192, 201, 217, 239, 240 244 and 292. Quantification of adamantanes, diamantanes and triamantanes was achieved by integration of peak heights with respect to the corresponding standards; D3 1-methyl-adamantane, D3 1-methyl-diamantane, and D4 triamantane, respectively. The quantification of tetramantanes was made relative to the D4 triamantane. D5 1-ethyl-diamantane was used to quantify ethyl-diamantanes. The quantification of steranes and hopanes were achieved by comparing the corresponding area with cholane using  $m/z$  217 and 191 respectively.

The following ions were monitored for aromatic hydrocarbon analysis:  $m/z$  119, 133, 191, 192, 219, 231, 245 and 253. The quantification of C<sub>26</sub> cholestane 20R, C<sub>27</sub> ergostane 20R and C<sub>28</sub> stigmastane 20R were achieved by using  $m/z$  231 with no standard.

## **2.6 Compound identification and calculation of diamondoid and biomarker parameters**

Compound identification was made by a combination of comparison with the standards, mass fragmentographic and relative retention times. PeakView version 1.2 was used to calculate

the height and the area of each peak. Diamondoid and biomarker concentrations were calculated based on comparing the appropriate standard peak with the peak of interest.

Pristane/phytane, pristane/ $nC_{17}$  and phytane/ $nC_{18}$  were determined by using GC-FID fragmentogram. Biodegradation was also investigated by comparing the relative amounts of these biomarkers; *n*-paraffins, isoprenoids, steranes, hopanes and diasteranes.

## 2.7 Data interpretation

Integrating all diamondoid and biomarker data to reveal the oil fields that contain inputs from deep cracked sources and to compare the parameters of the San Joaquin and Santa Barbara Basins in terms of the types of oil, maturity levels, depositional environment, source inputs, and biodegradation.

# CHAPTER III

## RESULT AND INTERPRETATION

### 3.1 Diamondoids

Petroleum from multiple sources resulted from a mixture of hydrocarbons generated and expelled at various degrees of thermal maturity. Because biomarkers from lower maturity sources dominate, source information from higher maturity oils and condensates is likely to be overlooked. Diamondoids appear to provide trustworthy data about high maturity petroleum because they are thermally very stable. Dahl *et al.* (1999) proposed a diamondoid-biomarker method based on their concentrations to determine thermal maturity for any oils and condensates at any maturity level. The method has been proved to be a useful tool in estimating the thermal maturity of both oils and condensates and can be used in the identification of mixed petroleum sources.

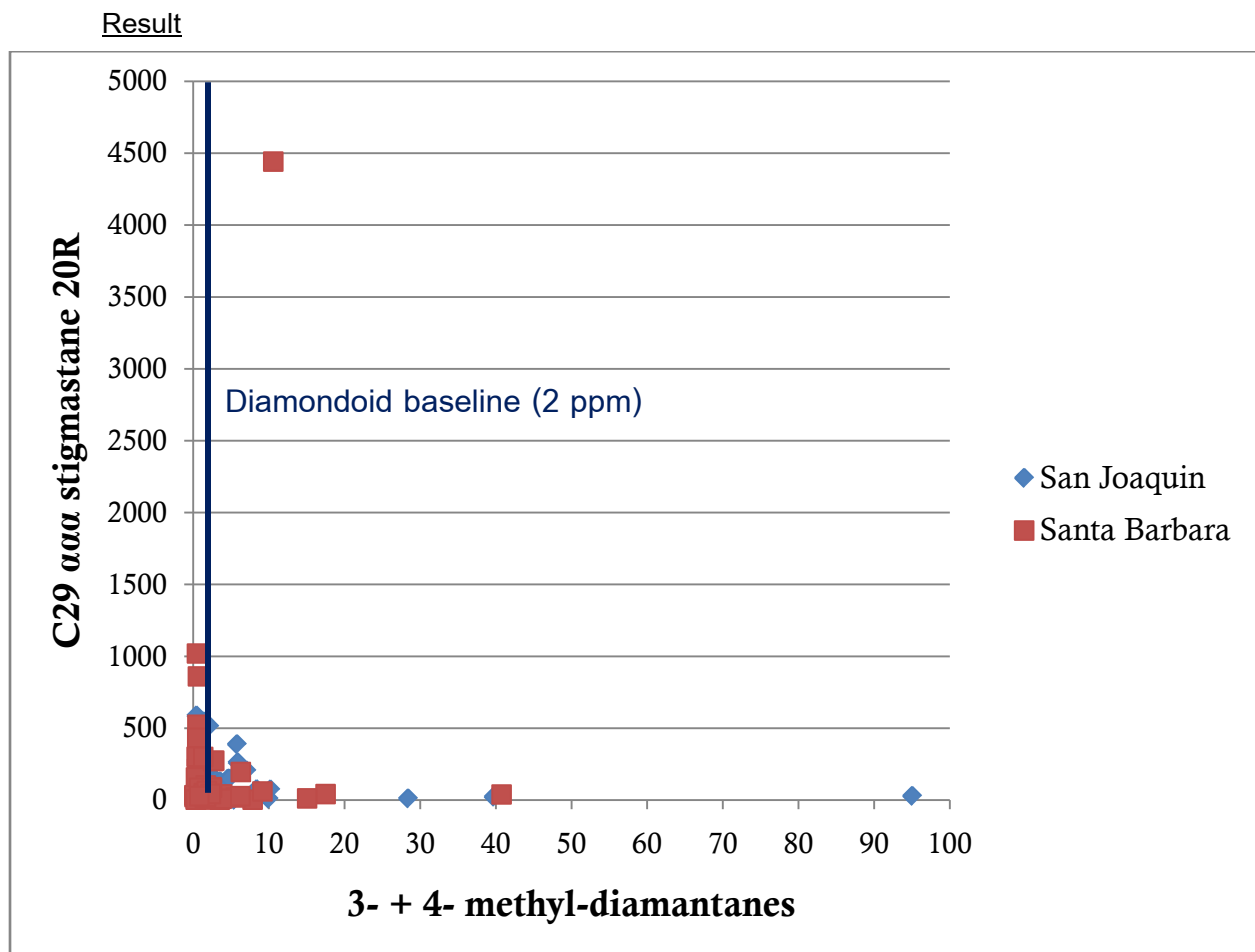


Figure 3.1: The relationship between 3- + 4- methyl-diamantanes and C<sub>29</sub> ααα stigmastane 20R in oil from the San Joaquin and Santa Barbara Basins showing the diamondoid baseline.

In Figure 3.1, it is noticeable that a few samples (red alphabets in Table 3.1) from the San Joaquin and Santa Barbara Basins have very high diamondoid concentrations. Results of these samples suggest that there should be at least one reservoir located deeper in these two basins which maintain oils with high diamondoid concentrations. Moreover, there should also be at least one reservoir located in a shallower area contributing to oils with moderate to high biomarker concentrations because most oil samples from these two basins are uncracked oils. A total of 47 oil samples from the San Joaquin Basin can be classified into 3 groups: (1) 18 samples are moderate to high maturity uncracked oils, (2) 24 samples are slightly cracked oils mixed with high maturity uncracked oils, and (3) 5 samples are intensely cracked oils mixed with high maturity uncracked oils. For the Santa Barbara Basin, 42 oil samples can be categorized into 4 groups: (1) 24 samples are moderate to high maturity uncracked oils, (2) 14 samples are slightly cracked oils mixed with high maturity uncracked oils, (3) 3 samples are extremely cracked oils mixed with high maturity uncracked oils, and (4) 1 sample is extremely cracked oil mixed with very low maturity uncracked oil. Therefore, it can be primarily concluded that some areas in the San Joaquin and Santa Barbara Basins have contributions from both shallow and deep reservoirs.

Samples	Adamantane (ppm)	3- + 4- methyl-diamantanes (ppm)	C <sub>29</sub> <b>ααα</b> stigmastane 20R (ppm)
MP-001	35.3	2.7	151.8
MP-002	11.3	1.0	232.3
MP-003	35.2	3.4	120.9
MP-004	43.3	3.0	139.5
MP-005	10.6	1.5	305.4
MP-006	91.0	10.2	73.6
MP-007	1014.0	95.0	28.7
MP-008	26.3	1.8	86.2
MP-009	17.0	2.1	513.8
MP-010	50.4	7.0	205.5
MP-011	0.5	1.1	35.0

**Table 3.1:** Concentrations of adamantane, 3- + 4- methyl-diamantanes and C<sub>29</sub> **ααα** stigmastane 20R in oil from the San Joaquin (gray boxes) and Santa Barbara (blue boxes) Basins.

Samples	Adamantane (ppm)	3- + 4- methyl-diamantanes (ppm)	C <sub>29</sub> $\alpha\alpha\alpha$ stigmastane 20R (ppm)
MP-012	12.1	5.8	388.9
MP-013	51.6	5.9	262.2
MP-014	67.0	8.4	75.3
MP-015	26.0	3.4	35.1
MP-016	32.4	3.0	104.4
MP-017	25.7	4.6	148.8
MP-018	25.2	2.5	92.3
MP-019	61.9	5.4	1.1
MP-020	36.7	3.9	5.6
MP-021	9.2	0.7	66.0
MP-022	15.9	1.7	272.2
MP-023	3.4	0.5	215.1
MP-024	18.4	2.6	22.0
MP-025	20.9	2.7	5.1
MP-026	9.2	1.3	231.8
MP-027	16.9	2.0	23.7
MP-028	16.6	3.6	90.7
MP-029	0.6	0.2	12.3
MP-030	6.9	1.0	98.1
MP-031	20.9	4.6	1.7
MP-032	93.8	28.4	11.3
MP-033	15.7	3.6	129.8
MP-034	9.3	1.0	151.2
MP-035	9.0	0.7	186.9
MP-036	153.9	39.7	22.9
MP-037	4.3	1.1	46.9

Table 3.1 (continued): Concentrations of adamantane, 3- + 4- methyl-diamantanes and C<sub>29</sub>  $\alpha\alpha\alpha$  stigmastane 20R in oil from the San Joaquin (gray boxes) and Santa Barbara (blue boxes) Basins.



Samples	Adamantane (ppm)	3- + 4- methyl-diamantanes (ppm)	C <sub>29</sub> $\alpha\alpha\alpha$ stigmastane 20R (ppm)
MP-038	71.2	10.0	9.4
MP-039	12.1	2.3	79.6
MP-040	6.3	0.5	107.9
MP-041	0.1	4.8	149.9
MP-042	24.9	2.9	7.6
MP-043	0.2	0.4	588.8
MP-044	0.1	3.2	64.2
MP-045	0.3	0.7	330.2
MP-046	3.7	2.7	66.2
MP-047	7.6	1.5	547.1
MP-048	4.4	1.4	5.1
MP-049	26.0	2.4	89.4
MP-050	7.3	17.5	41.9
MP-051	4.2	40.8	38.9
MP-052	39.5	7.8	2.7
MP-053	0.9	15.1	12.0
MP-054	0.2	2.2	8.2
MP-055	2.5	1.2	4.6
MP-056	2.4	0.4	4.3
MP-057	1.1	0.2	24.5
MP-058	6.0	0.5	219.3
MP-059	0.8	0.2	20.2
MP-060	3.8	0.4	158.2
MP-061	9.5	1.7	102.2
MP-062	0.7	0.1	34.1
MP-063	2.2	1.5	15.6

Table 3.1 (continued): Concentrations of adamantane, 3- + 4- methyl-diamantanes and C<sub>29</sub>  $\alpha\alpha\alpha$  stigmastane 20R in oil from the San Joaquin (gray boxes) and Santa Barbara (blue boxes) Basins.

Samples	Adamantane (ppm)	3- + 4- methyl-diamantanes (ppm)	C <sub>29</sub> <b>ααα</b> stigmastane 20R (ppm)
MP-064	41.6	3.8	39.3
MP-065	0.3	9.1	60.0
MP-066	1.8	1.3	45.6
MP-067	3.5	0.5	523.9
MP-068	2.9	0.5	432.7
MP-069	3.4	0.6	860.4
MP-070	3.0	0.4	301.5
MP-071	5.4	5.6	17.7
MP-072	29.7	2.6	270.8
MP-073	57.5	3.5	2.7
MP-074	26.6	2.8	274.4
MP-075	1.0	1.3	300.2
MP-076	15.7	6.3	195.1
MP-077	0.1	3.8	9.1
<b>MP-078</b>	<b>4.9</b>	<b>10.6</b>	<b>4442.6</b>
MP-079	3.7	0.5	1019.6
MP-080	0.6	0.3	2.6
MP-081	0.6	0.8	85.8
MP-082	1.9	1.5	7.9
MP-083	2.5	6.2	27.0
MP-084	1.2	1.7	22.1
MP-085	4.0	2.5	85.9
MP-086	1.2	1.4	47.4
MP-087	0.9	1.8	62.8
MP-088	1.1	2.3	42.6
MP-089	0.1	0.8	27.5

Table 3.1 (continued): Concentrations of adamantane, 3- + 4- methyl diamantanes and C<sub>29</sub> **ααα** stigmastane 20R in oil from the San Joaquin (gray boxes) and Santa Barbara (blue boxes) Basins.

## 3.2 Biomarkers

### 3.2.1 Pristane/phytane ratio

Pristane (Pr) and phytane (Ph) are isoprenoid hydrocarbons with the formula  $C_{19}H_{40}$  and  $C_{20}H_{42}$ , respectively. They are primarily derived from the side chain of chlorophyll in phototropic organisms. Pr/Ph ratio has been commonly used to indicate oxic or anoxic depositional environment of the source rocks generating petroleum. High Pr/Ph ratios ( $>3.0$ ) suggest terrestrial organic matter inputs within oxic conditions. On the other hand, low values of Pr/Ph ratios ( $<0.6$ ) imply anoxic and hypersaline environments. In addition, Pr/Ph ratios in the range 0.8-2.5 are not appropriate to use as an indicator of paleoenvironment alone without comparing with other corresponding parameters (Peters and Moldowan, 1993).

#### Result

Pr/Ph ratio of oil samples from the San Joaquin Basin are in the range of 0.62-3.53 as shown in Table 3.2 which indicate that (1) the deposition was in quasi-oxic to oxic environment and/or (2) samples are in fairly high maturity levels. MP-007 has the highest Pr/Ph ratio (3.53) which suggests contribution from terrestrial organic matter inputs under oxic condition. This sample also has the highest diamondoid concentration among samples analyzed in this research.

For oil samples from the Santa Barbara Basin, Pr/Ph ratios are in the range of 0.44-2.20 as shown in Table 3.2 which suggest that (1) source rocks were deposited in anoxic to sub-oxic environment and/or (2) samples are of relatively high maturity levels, the same as samples from the San Joaquin Basin. MP-071 has the highest Pr/Ph ratio (2.20) but it has fairly high diamondoid concentrations (5.6 ppm). However, MP-051 which has the highest diamondoid concentrations in the basin has low Pr/Ph ratio (0.84).

### 3.2.2 Pristane/ $nC_{17}$ and Phytane/ $nC_{18}$

Pristane with  $nC_{17}$  and phytane with  $nC_{18}$  can be easily identified from a gas chromatogram by their appearances with the distinctive doublet. Pristane/ $nC_{17}$  and phytane/ $nC_{18}$  are commonly used in petroleum correlation studies as a primary indicator of maturity levels, organic source inputs and biodegradation. These two ratios are less than 0.5 indicating high maturity oils and/or oils derived from anoxic environment. Whereas, low maturity oils and/or oils derived from oxic

condition have the ratios greater than 1.0. However, these two ratios should be used cautiously for many reasons such as biodegradation and thermal maturity (Peters and Moldowan, 1993).

### Result

Pristane/ $nC_{17}$  and phytane/ $nC_{18}$  ratios of oil samples from the San Joaquin Basin are quite high. There is one sample which has both ratios less than 0.5 and there are 13 samples which have ratios greater than 1 (Figure 3.2). The results may indicate that the deposition was in quasi-oxic to oxic environment and the samples are of fairly high level of biodegradation. The result also suggests that the source rocks may consist of type II-III kerogen mixtures.

Similar to oils from the San Joaquin Basin, there is one sample from the Santa Barbara Basin which has ratios less than 0.5 and there are 11 samples which have the ratios greater than 1. These may suggest that the oil samples were generated from source rocks deposited in quasi-oxic to oxic environment and they were rather severely biodegraded. Based on this plot, the kerogen types in source rocks are also somewhat the same to those of the San Joaquin Basin.

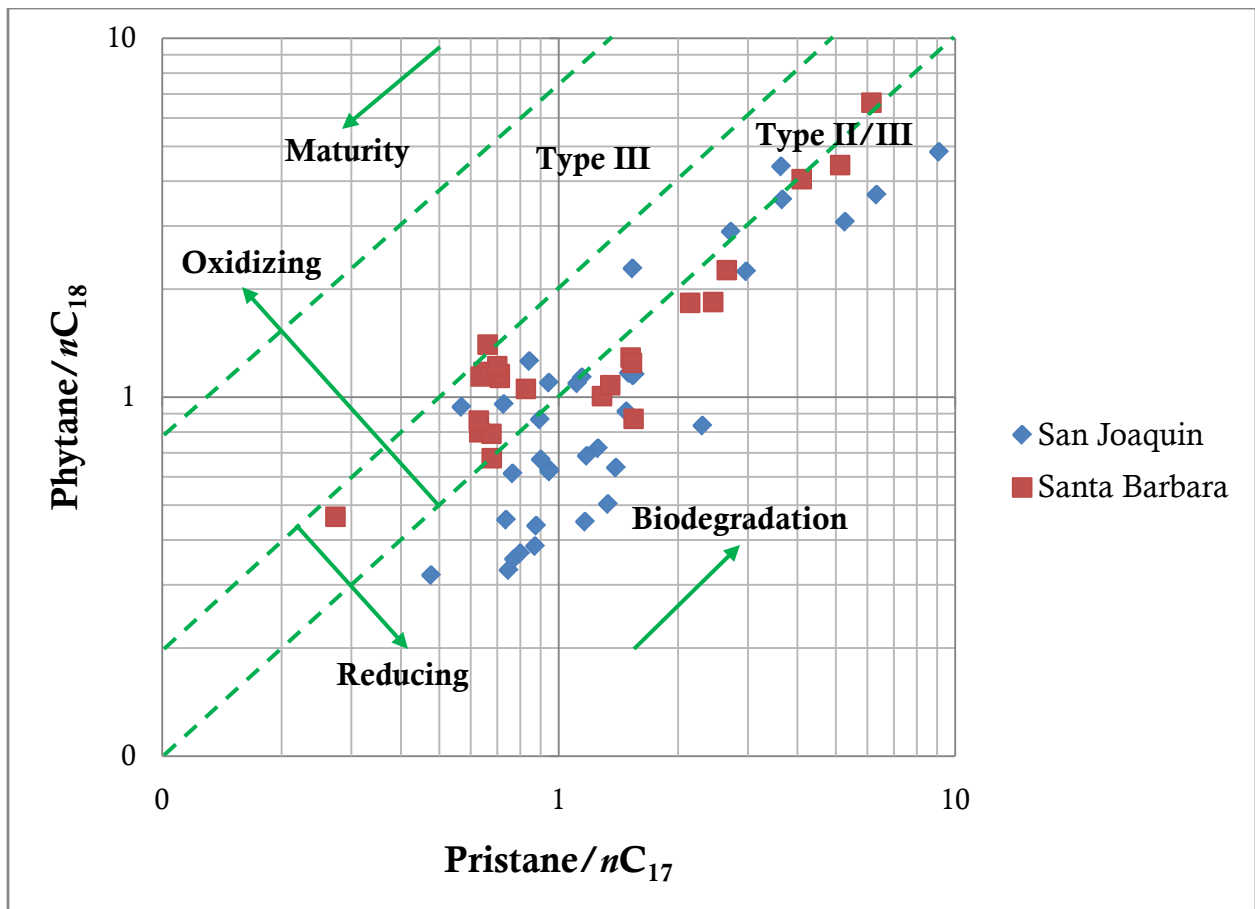


Figure 3.2: A crossplot of pristane/ $nC_{17}$  versus phytane/ $nC_{18}$ , plot modified from Shanmugam (1985).

Samples	Biodegradation rank	Pr/Ph	Pr/nC <sub>17</sub>	Ph/nC <sub>18</sub>	Ts/Tm	Ts/(Ts+Tm)
MP-001	0	1.70	0.95	0.62	1.28	0.56
MP-002	0	1.42	1.56	1.16	2.19	0.69
MP-003	2	0.90	3.64	4.39	3.32	0.77
MP-004	0	1.02	0.95	1.10	1.17	0.54
MP-005	0	1.85	5.28	3.08	1.09	0.52
MP-006	0	2.58	0.75	0.33	1.78	0.64
MP-007	1-2	3.53	2.30	0.83	1.02	0.50
MP-008	2	2.22	9.10	4.82	1.00	0.50
MP-009	0	1.90	6.33	3.67	1.16	0.54
MP-010	0	3.13	1.17	0.45	2.23	0.69
MP-011	6	N/A	N/A	N/A	1.06	0.51
MP-012	0	2.44	1.39	0.64	3.05	0.75
MP-013	0	2.88	1.33	0.50	2.36	0.70
MP-014	0	2.59	0.77	0.35	2.09	0.68
MP-015	0	2.56	0.80	0.37	2.15	0.68
MP-016	0	1.72	0.95	0.63	1.28	0.56
MP-017	0	1.72	0.95	0.62	1.26	0.56
MP-018	2	2.00	0.90	0.87	1.60	0.62
MP-019	6-7	N/A	N/A	N/A	0.14	0.12
MP-020	4-5	N/A	N/A	N/A	0.12	0.10
MP-021	1	1.38	3.67	3.56	2.20	0.69
MP-022	1	1.35	2.72	2.89	1.55	0.61
MP-023	0	0.84	0.73	0.96	8.48	0.89

N/A = not applicable

**Table 3.2:** The ratios of Pr/Ph, Pr/nC<sub>17</sub>, Ph/nC<sub>18</sub>, Ts/Tm and Ts/(Ts+Tm) with biodegradation ranks (based on Peters and Moldowan, 1993) of the oil samples from the San Joaquin (gray boxes) and Santa Barbara (blue boxes) Basins.

Samples	Biodegradation rank	Pr/Ph	Pr/nC <sub>17</sub>	Ph/nC <sub>18</sub>	Ts/Tm	Ts/(Ts+Tm)
MP-024	6-7	N/A	N/A	N/A	0.33	0.25
MP-025	6-7	N/A	N/A	N/A	0.16	0.14
MP-026	0	1.37	1.50	1.17	2.08	0.68
MP-027	6-7	N/A	N/A	N/A	0.59	0.37
MP-028	0	1.90	1.18	0.69	0.99	0.50
MP-029	1	0.62	0.57	0.94	6.12	0.86
MP-030	0	0.69	0.84	1.26	6.26	0.86
MP-031	6-7	N/A	N/A	N/A	5.78	0.85
MP-032	0	1.89	0.48	0.32	0.93	0.48
MP-033	0	1.53	0.90	0.67	1.02	0.51
MP-034	0	1.08	1.14	1.14	7.90	0.89
MP-035	0	1.50	2.97	2.24	1.81	0.64
MP-036	0	2.72	0.87	0.38	0.83	0.45
MP-037	0	1.35	0.77	0.61	2.47	0.71
MP-038	6-7	N/A	N/A	N/A	0.88	0.47
MP-039	0	2.05	1.26	0.72	1.23	0.55
MP-040	0	1.10	1.11	1.09	14.01	0.93
MP-041	0	2.29	0.88	0.44	1.13	0.53
MP-042	6-7	N/A	N/A	N/A	2.20	0.69
MP-043	1-2	0.64	1.54	2.28	5.26	0.84
MP-044	6-8	N/A	N/A	N/A	4.97	0.83
MP-045	0	1.88	1.48	0.91	5.37	0.84
MP-046	0	1.94	0.74	0.46	4.97	0.83

N/A = not applicable

**Table 3.2 (continued):** The ratios of Pr/Ph, Pr/nC<sub>17</sub>, Ph/nC<sub>18</sub>, Ts/Tm and Ts/(Ts+Tm) with biodegradation ranks (based on Peters and Moldowan, 1993) of the oil samples from the San Joaquin (gray boxes) and Santa Barbara (blue boxes) Basins.

Samples	Biodegradation rank	Pr/Ph	Pr/nC <sub>17</sub>	Ph/nC <sub>18</sub>	Ts/Tm	Ts/(Ts+Tm)
MP-047	0	2.20	1.54	1.15	9.13	0.90
MP-048	8	N/A	N/A	N/A	4.08	0.80
MP-049	6-7	N/A	N/A	N/A	0.56	0.36
MP-050	0	1.10	0.68	0.68	21.61	0.96
MP-051	0	0.84	0.63	0.80	40.44	0.98
MP-052	6-8	N/A	N/A	N/A	13.39	0.93
MP-053	6-8	N/A	N/A	N/A	12.48	0.93
MP-054	6-8	N/A	N/A	N/A	0.71	0.41
MP-055	6-8	N/A	N/A	N/A	80.94	0.99
MP-056	6-8	N/A	N/A	N/A	30.58	0.97
MP-057	0	0.54	0.65	1.18	16.79	0.94
MP-058	0	1.27	2.45	1.84	12.95	0.93
MP-059	0	0.54	0.64	1.14	44.72	0.98
MP-060	0	1.26	1.52	1.29	16.03	0.94
MP-061	6-8	N/A	N/A	N/A	2.17	0.68
MP-062	1	0.44	0.66	1.40	25.74	0.96
MP-063	1	1.33	1.53	1.25	33.06	0.97
MP-064	6-8	N/A	N/A	N/A	0.96	0.49
MP-065	1	1.31	1.29	1.01	0.86	0.46
MP-066	0	0.62	0.27	0.46	0.77	0.44
MP-067	1	1.18	2.15	1.83	4.86	0.83
MP-068	1-2	1.22	6.15	6.62	0.88	0.47
MP-069	1-2	1.19	2.65	2.26	2.18	0.69

N/A = not applicable

**Table 3.2 (continued):** The ratios of Pr/Ph, Pr/nC<sub>17</sub>, Ph/nC<sub>18</sub>, Ts/Tm and Ts/(Ts+Tm) with biodegradation ranks (based on Peters and Moldowan, 1993) of the oil samples from the San Joaquin (gray boxes) and Santa Barbara (blue boxes) Basins.

Samples	Biodegradation rank	Pr/Ph	Pr/nC <sub>17</sub>	Ph/nC <sub>18</sub>	Ts/Tm	Ts/(Ts+Tm)
MP-070	1	1.23	4.10	4.05	5.36	0.84
MP-071	1	2.20	1.54	0.87	2.50	0.71
MP-072	6-8	N/A	N/A	N/A	21.39	0.96
MP-073	6-8	N/A	N/A	N/A	18.33	0.95
MP-074	6-8	N/A	N/A	N/A	24.18	0.96
MP-075	6-8	N/A	N/A	N/A	11.03	0.92
MP-076	0	0.93	0.68	0.79	11.16	0.92
MP-077	8	N/A	N/A	N/A	15.14	0.94
MP-078	1-2	1.25	5.13	4.43	15.00	0.94
MP-079	0	1.38	1.35	1.08	18.28	0.95
MP-080	8	N/A	N/A	N/A	2.16	0.68
MP-081	8	N/A	N/A	N/A	1.00	0.50
MP-082	8	N/A	N/A	N/A	54.83	0.98
MP-083	8	N/A	N/A	N/A	1.87	0.65
MP-084	0	0.77	0.63	0.86	0.82	0.45
MP-085	0	0.80	0.83	1.05	0.59	0.37
MP-086	0	0.63	0.71	1.13	3.47	0.78
MP-087	1-2	0.79	0.71	1.16	1.34	0.57
MP-088	0	0.59	0.70	1.22	3.13	0.76
MP-089	8	N/A	N/A	N/A	1.56	0.61

N/A = not applicable

**Table 3.2 (continued):** The ratios of Pr/Ph, Pr/nC<sub>17</sub>, Ph/nC<sub>18</sub>, Ts/Tm and Ts/(Ts+Tm) with biodegradation ranks (based on Peters and Moldowan, 1993) of the oil samples from the San Joaquin (gray boxes) and Santa Barbara (blue boxes) Basins.

### 3.2.3 Ts/(Ts+Tm)

The ratio of trisnorneohopane (Ts, C<sub>27</sub>H<sub>46</sub>) to trisnorhopane (Tm, C<sub>27</sub>H<sub>46</sub>) can be used as the reliable maturity indicator if oils being evaluated are from a common source of consistent organic



facies. However, Ts and Tm sometimes commonly coelute with tricyclic or tetracyclic terpanes on the  $m/z$  191 mass chromatogram, so the  $Ts/(Ts+Tm)$  ratio should be used carefully. The  $Ts/(Ts+Tm)$  ratio about 1.0 indicate the base of the oil window (Peters and Moldowan, 1993).

### Result

A crossplot of  $Ts/Tm$  versus  $Ts/(Ts+Tm)$  ratio of oil samples from the San Joaquin Basin is very disperse as shown in Figure 3.3 which suggests that the samples consist of moderate to high maturity oils. This result may suggest that these oil samples were generated from the same source rocks in the basin with variation in maturity levels.

For the oil samples from the Santa Barbara Basin, the crossplot is also scattered and has the same trend line as the samples from the San Joaquin Basin, but the samples from the Santa Barbara Basin have slightly higher maturity. This result may indicate that these two basins have fairly the same organic input facies, however, samples with  $Ts/Tm$  ratio higher than 20 are not reliable because they may be coeluted with other compounds.

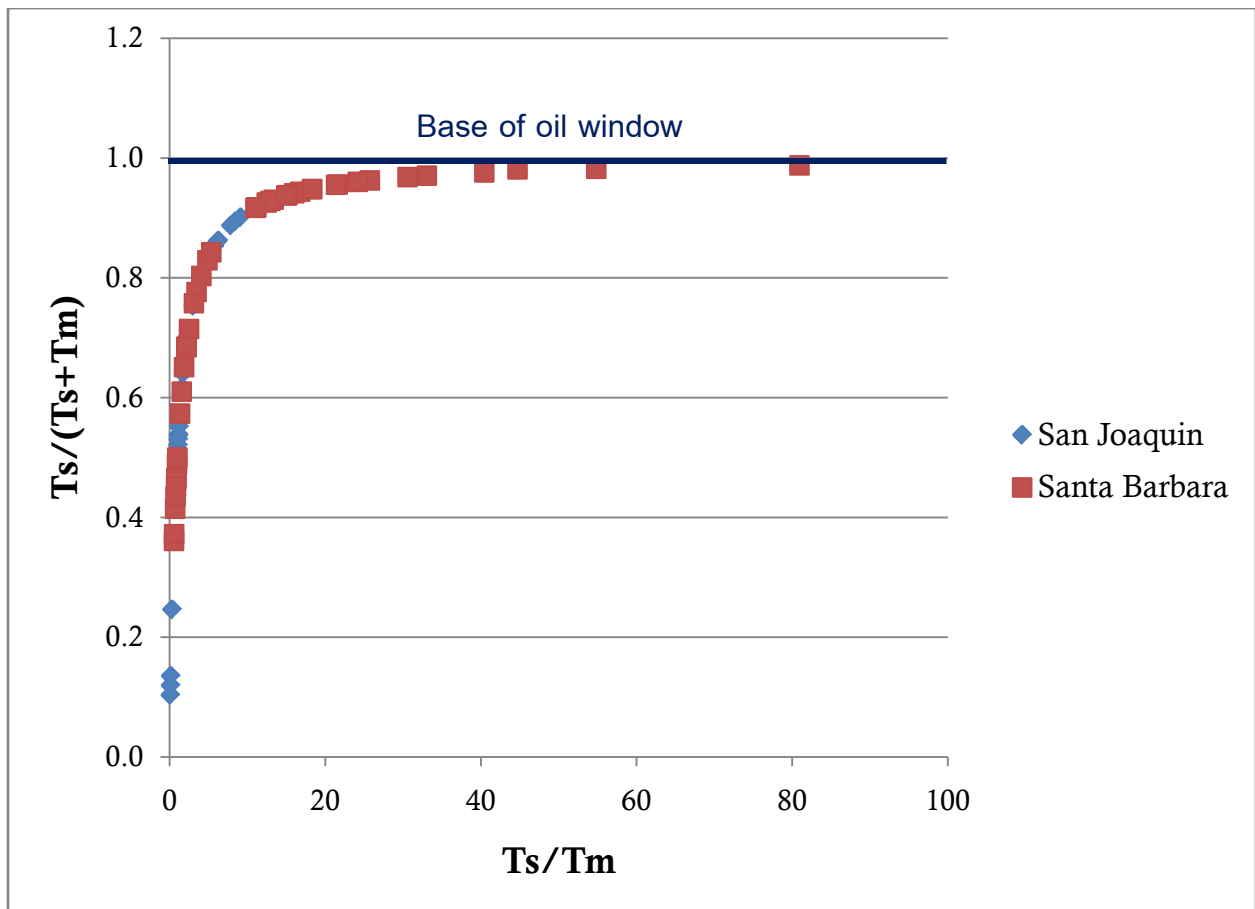


Figure 3.3: A Crossplot of  $Ts/Tm$  versus  $Ts/(Ts+Tm)$ .

### 3.2.4 Oleananes and oleanane index

Oleananes are derived from only some angiosperms (flowering plants), so they are used as important markers for higher plant inputs. If oleananes are detectable in oil, the source rocks must be in Cretaceous or younger. In addition, if oleanane index (oleananes/hopane) is greater than 0.2, the source rock should probably be Tertiary in age (Moldowan *et al.*, 1994).

#### Result

Oleananes were found in every oil sample from both the San Joaquin and Santa Barbara Basins indicating that the samples were generated from Cretaceous-Tertiary source rocks. Oleanane indexes of 5 samples from the San Joaquin Basin (Table 3.3) are greater than 0.2, but three of them are not reliable because the oils are biodegraded leading to relatively low hopane. Whereas, 11 oil samples from the Santa Barbara Basin have indexes of more than 0.2 (Table 3.3), but six of them were severely biodegraded so the indexes are not trustworthy. Therefore, the oleanane indexes of these two basins merely indicate that the oils originated from the Cretaceous source rocks.

Samples	Oleanane index	C <sub>31</sub> [22S/(22S+22R)]	C <sub>32</sub> [22S/(22S+22R)]	Gammacerane	C <sub>35</sub> Homohopane
MP-001	0.09	0.59	0.56	Yes	Yes
MP-002	0.13	0.57	0.55	Yes	Yes
MP-003	0.28	0.57	0.58	Yes	Yes
MP-004	0.09	0.57	0.56	Yes	Yes
MP-005	0.05	0.53	0.51	Yes	Yes
MP-006	0.13	0.59	0.56	Yes	Yes
MP-007	0.04	0.59	0.57	Yes	Yes
MP-008	0.05	0.58	0.57	Yes	Yes
MP-009	0.05	0.53	0.51	Yes	Yes
MP-010	0.18	0.44	0.52	Yes	Yes
MP-011	0.22	0.52	0.59	Yes	Yes

**Table 3.3:** Oleanane index, homohopane isomerization ratios, gammacerane and C<sub>35</sub> homohopane of the oil samples from the San Joaquin (gray boxes) and Santa Barbara (blue boxes) Basins.

Samples	Oleanane index	C <sub>31</sub> [22S/(22S+22R)]	C <sub>32</sub> [22S/(22S+22R)]	Gammacerane	C <sub>35</sub> Homohopane
MP-012	0.17	0.50	0.53	Yes	Yes
MP-013	0.18	0.47	0.53	Yes	Yes
MP-014	0.15	0.57	0.56	Yes	Yes
MP-015	0.15	0.57	0.55	Yes	Yes
MP-016	0.10	0.58	0.56	Yes	Yes
MP-017	0.09	0.58	0.56	Yes	Yes
MP-018	0.18	0.56	0.53	Yes	Yes
MP-019	0.83	0.63	0.48	Yes	Yes
MP-020	0.82	0.69	0.52	Yes	Yes
MP-021	0.16	0.55	0.52	Yes	Yes
MP-022	0.10	0.57	0.51	Yes	Yes
MP-023	0.09	0.58	0.56	Yes	Yes
MP-024	0.09	0.69	0.51	Yes	Yes
MP-025	0.73	0.55	0.57	Yes	Yes
MP-026	0.13	0.58	0.55	Yes	Yes
MP-027	0.20	0.47	0.54	Yes	Yes
MP-028	0.21	0.44	0.55	Yes	Yes
MP-029	0.10	0.58	0.59	Yes	Yes
MP-030	0.05	0.59	0.59	Yes	Yes
MP-031	1.56	0.52	0.55	Yes	Yes
MP-032	0.03	0.57	0.57	Yes	Yes
MP-033	0.10	0.58	0.56	Yes	Yes
MP-034	0.08	0.57	0.57	Yes	Yes
MP-035	0.18	0.58	0.52	Yes	Yes
MP-036	0.25	0.59	0.58	Yes	Yes
MP-037	0.15	0.59	0.58	Yes	Yes

**Table 3.3 (continued):** Oleanane index, homohopane isomerization ratios, gammacerane and C<sub>35</sub>

homohopane of the oil samples from the San Joaquin (gray boxes) and Santa Barbara (blue boxes) Basins.

Samples	Oleanane index	C <sub>31</sub> [22S/(22S+22R)]	C <sub>32</sub> [22S/(22S+22R)]	Gammacerane	C <sub>35</sub> Homohopane
MP-038	0.50	0.60	0.57	Yes	Yes
MP-039	0.14	0.58	0.56	Yes	Yes
MP-040	0.15	0.58	0.58	Yes	Yes
MP-041	0.17	0.58	0.56	Yes	Yes
MP-042	0.11	0.56	0.54	Yes	Yes
MP-043	0.10	0.55	0.55	Yes	Yes
MP-044	0.08	0.56	0.54	Yes	Yes
MP-045	0.10	0.56	0.55	Yes	Yes
MP-046	0.11	0.57	0.56	Yes	Yes
MP-047	0.23	0.63	0.62	Yes	Yes
MP-048	0.59	0.59	0.57	Yes	Yes
MP-049	0.05	0.56	0.57	Yes	Yes
MP-050	0.08	0.56	0.57	Yes	Yes
MP-051	0.06	0.58	0.56	Yes	Yes
MP-052	0.11	0.58	0.58	Yes	Yes
MP-053	0.07	0.56	0.56	Yes	Yes
MP-054	0.04	0.57	0.55	Yes	Yes
MP-055	0.06	0.56	0.59	Yes	Yes
MP-056	0.06	0.56	0.56	Yes	Yes
MP-057	0.06	0.58	0.58	Yes	Yes
MP-058	0.10	0.56	0.55	Yes	Yes
MP-059	0.08	0.59	0.59	Yes	Yes
MP-060	0.11	0.56	0.56	Yes	Yes
MP-061	0.07	0.58	0.56	Yes	Yes
MP-062	0.10	0.58	0.59	Yes	Yes
MP-063	0.07	0.57	0.59	Yes	Yes

**Table 3.3 (continued):** Oleanane index, homohopane isomerization ratios, gammacerane and C<sub>35</sub>

homohopane of the oil samples from the San Joaquin (gray boxes) and Santa Barbara (blue boxes) Basins.

Samples	Oleanane index	C <sub>31</sub> [22S/(22S+22R)]	C <sub>32</sub> [22S/(22S+22R)]	Gammacerane	C <sub>35</sub> Homohopane
MP-064	0.05	0.58	0.56	Yes	Yes
MP-065	0.22	0.43	0.40	Yes	Yes
MP-066	0.13	0.55	0.56	Yes	Yes
MP-067	0.28	0.53	0.52	Yes	Yes
MP-068	0.15	0.56	0.55	Yes	Yes
MP-069	0.08	0.54	0.58	Yes	Yes
MP-070	0.10	0.59	0.54	Yes	Yes
MP-071	0.10	0.56	0.53	Yes	Yes
MP-072	0.09	0.58	0.60	Yes	Yes
MP-073	0.47	0.58	0.57	Yes	Yes
MP-074	0.08	0.58	0.59	Yes	Yes
MP-075	0.09	0.56	0.58	Yes	Yes
MP-076	0.08	0.58	0.60	Yes	Yes
MP-077	0.06	0.58	0.61	Yes	Yes
MP-078	0.07	0.59	0.58	Yes	Yes
MP-079	0.05	0.57	0.61	Yes	Yes
MP-080	0.37	0.48	0.52	Yes	Yes
MP-081	0.31	0.45	0.45	Yes	Yes
MP-082	0.05	0.57	0.58	Yes	Yes
MP-083	0.21	0.57	0.54	Yes	Yes
MP-084	0.13	0.59	0.58	Yes	Yes
MP-085	0.15	0.59	0.59	Yes	Yes
MP-086	0.12	0.58	0.57	Yes	Yes
MP-087	0.07	0.58	0.56	Yes	Yes
MP-088	0.89	0.59	0.56	Yes	Yes
MP-089	0.07	0.57	0.57	Yes	Yes

**Table 3.3 (continued):** Oleanane index, homohopane isomerization ratios, gammacerane and C<sub>35</sub>

homohopane of the oil samples from the San Joaquin (gray boxes) and Santa Barbara (blue boxes) Basins.

### 3.2.5 Homohopane isomerization

Hopanes are classified as pentacyclic hydrocarbons. The origin of the hopanes is the most abundant hopanoid in prokaryotes. The C-22 position in the  $C_{31}$  to  $C_{35}$  is chiral carbon which is characteristic as R and S doublets in  $m/z$  191 mass chromatogram. Homohopane isomerization ratios  $[22S/(22S+22R)]$  are often used to determine maturity levels, especially  $C_{31}$  and  $C_{32}$  homohopanes. When the samples have the ratios in the range 0.50-0.54, this suggests the maturity level of the top of the oil window. Whereas, the ratios in the range 0.57-0.62 suggest that they already reached the peak of the oil window (Seifert and Moldowan, 1986).

#### Result

A crossplot of  $C_{31}[22S/(22S+22R)]$  and  $C_{32}[22S/(22S+22R)]$  ratios of the oil samples from both San Joaquin and Santa Barbara Basins (Figure 3.4) indicates that most oil samples are of fairly high maturity and nearly reach the peak of the oil window. Intensely cracked oil samples do not have a difference in the ratios from the others. This result may suggest the intensely cracked oils migrated from more than one source with at least one of them consisting of non-cracked oils.

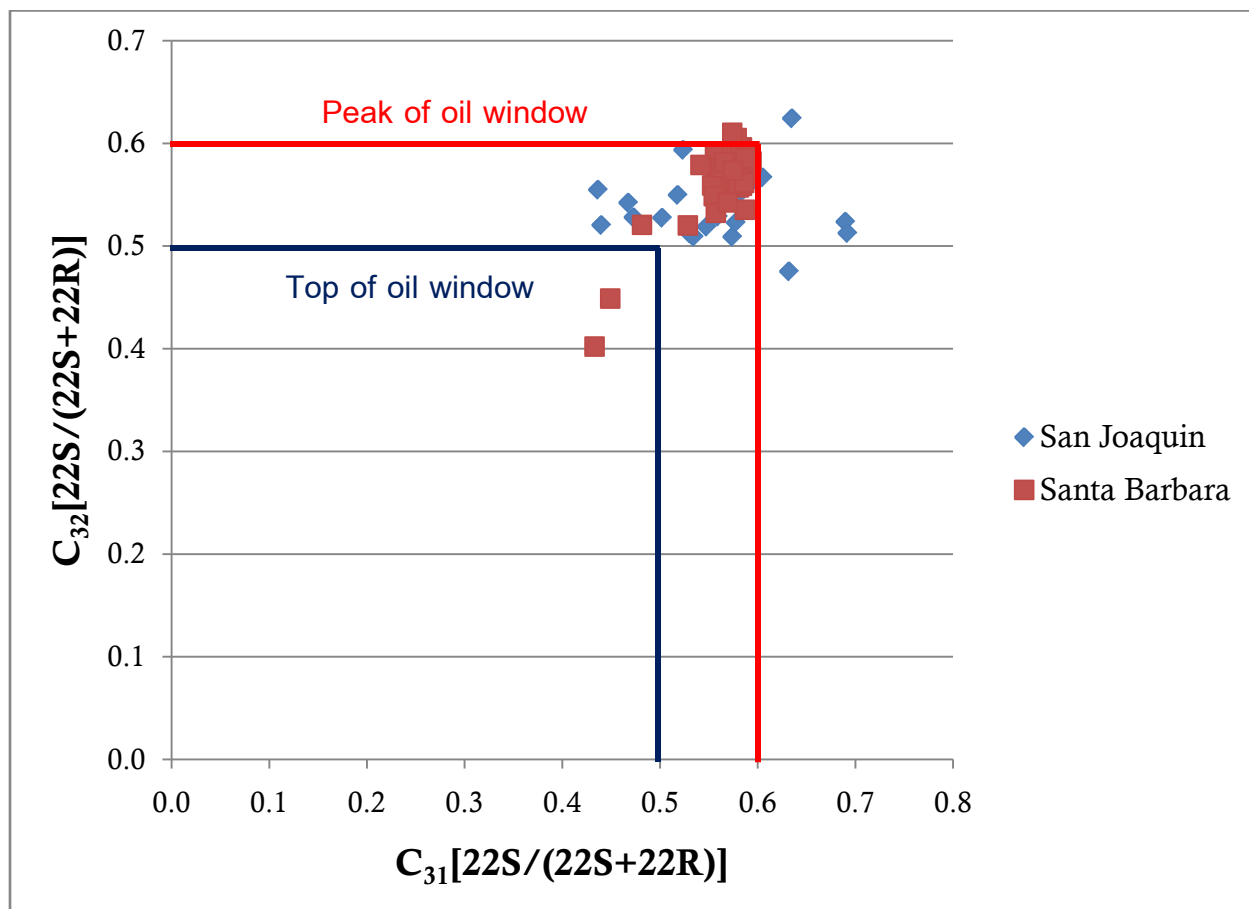


Figure 3.4: A crossplot of  $C_{31}[22S/(22S+22R)]$  versus  $C_{32}[22S/(22S+22R)]$ .

### 3.2.6 Gammacerane

Gammacerane is a pentacyclic triterpane with formula  $C_{30}H_{52}$  and can be measured on  $m/z$  191 mass chromatogram. It is often used to represent hypersaline depositional environments. It is also found in many lacustrine oils and bitumen as a main biomarker. Although oils and bitumen with high gammacerane can point to a hypersaline depositional environment, this environment does not always need to have high gammacerane (Moldowan *et al.*, 1985; Peters and Moldowan, 1993).

#### Result

All oil samples from both San Joaquin and Santa Barbara Basins contain gammacerane as shown in Table 3.3. This result may indicate that source rocks of both basins were deposited in hypersaline marine or lacustrine environment.

### 3.2.7 $C_{35}$ homohopane

$C_{35}$  homohopane can indicate the degree of oxicity which sediments were deposited. When oil and bitumen samples contain high  $C_{35}$  homohopane, it suggests that those samples were generated from the source rocks which were likely deposited in hypersaline environment (Peters *et al.*, 2005).

#### Result

Table 3.3 shows that  $C_{35}$  homohopane is commonly found in every oil sample from both San Joaquin and Santa Barbara Basins. This result may suggest that source rocks in these two basins were deposited in hypersaline environment.

### 3.2.8 $n$ -alkane distributions

The  $n$ -alkane chromatographic profile has been used primarily as a marker for source rock's depositional environment and source of organic inputs.  $nC_{15}$ ,  $nC_{17}$ , and  $nC_{19}$  are mostly originated from algae in lacustrine and marine environments. Whereas, land plants in terrestrial environment produced generally  $nC_{27}$ ,  $nC_{29}$ , and  $nC_{31}$ . Moreover, if the distribution is dominated by  $nC_{23}$ ,  $nC_{25}$ ,  $nC_{27}$ ,  $nC_{29}$ , and  $nC_{31}$ , it suggests that source is from non-marine algae in lacustrine environment (Volkman, 1988). The  $n$ -alkane distribution can be identified in GC-FID.

#### Result

The  $n$ -alkane distributions of all samples from the San Joaquin Basin are in range from  $C_{13}$  to  $C_{31}$  and mostly in  $C_{13}$ ,  $C_{15}$ ,  $C_{17}$ , and  $C_{19}$  as shown in Figure 3.5. Therefore, they may indicate that

the major organic input in this basin is algae. In addition, they also contain some inputs from land plants which may indicate that source rocks of the San Joaquin Basin were deposited in shallow marine environment not far from the continent.

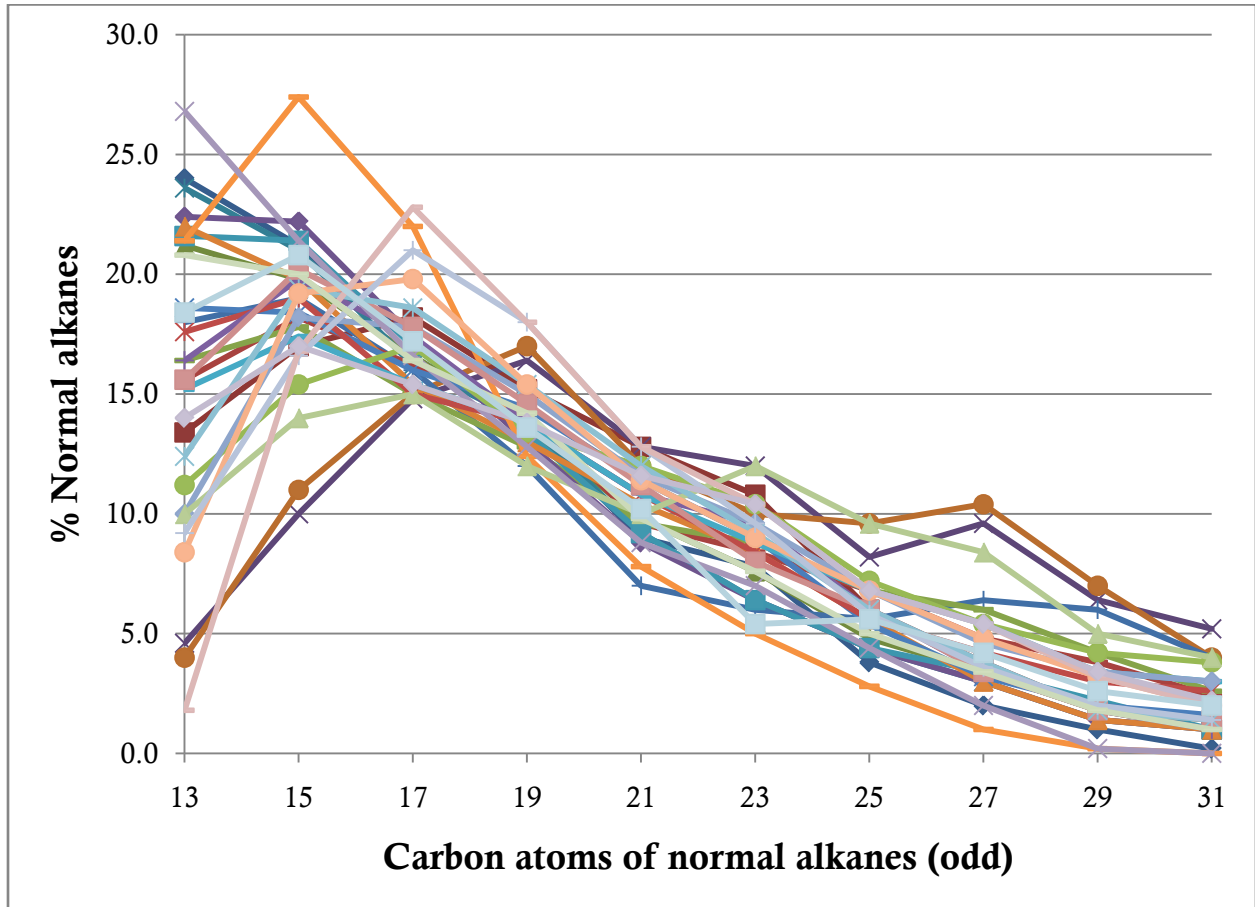


Figure 3.5: *n*-alkane distributions of non-biodegraded oil samples from the San Joaquin Basin.

All samples from the Santa Barbara Basin have *n*-alkane distributions ranging from C<sub>13</sub> to C<sub>31</sub> and maximize in C<sub>13</sub>, C<sub>15</sub>, C<sub>17</sub>, and C<sub>19</sub> (Figure 3.6) which is similar to oils from the San Joaquin Basin. In comparison, it is noticeable that oil samples from the Santa Barbara Basin have more algae and less land plant inputs than the San Joaquin Basin's oil. Therefore, they may suggest that the Santa Barbara Basin's source rocks were deposited deeper part of shallow marine environment than those of the San Joaquin Basin.



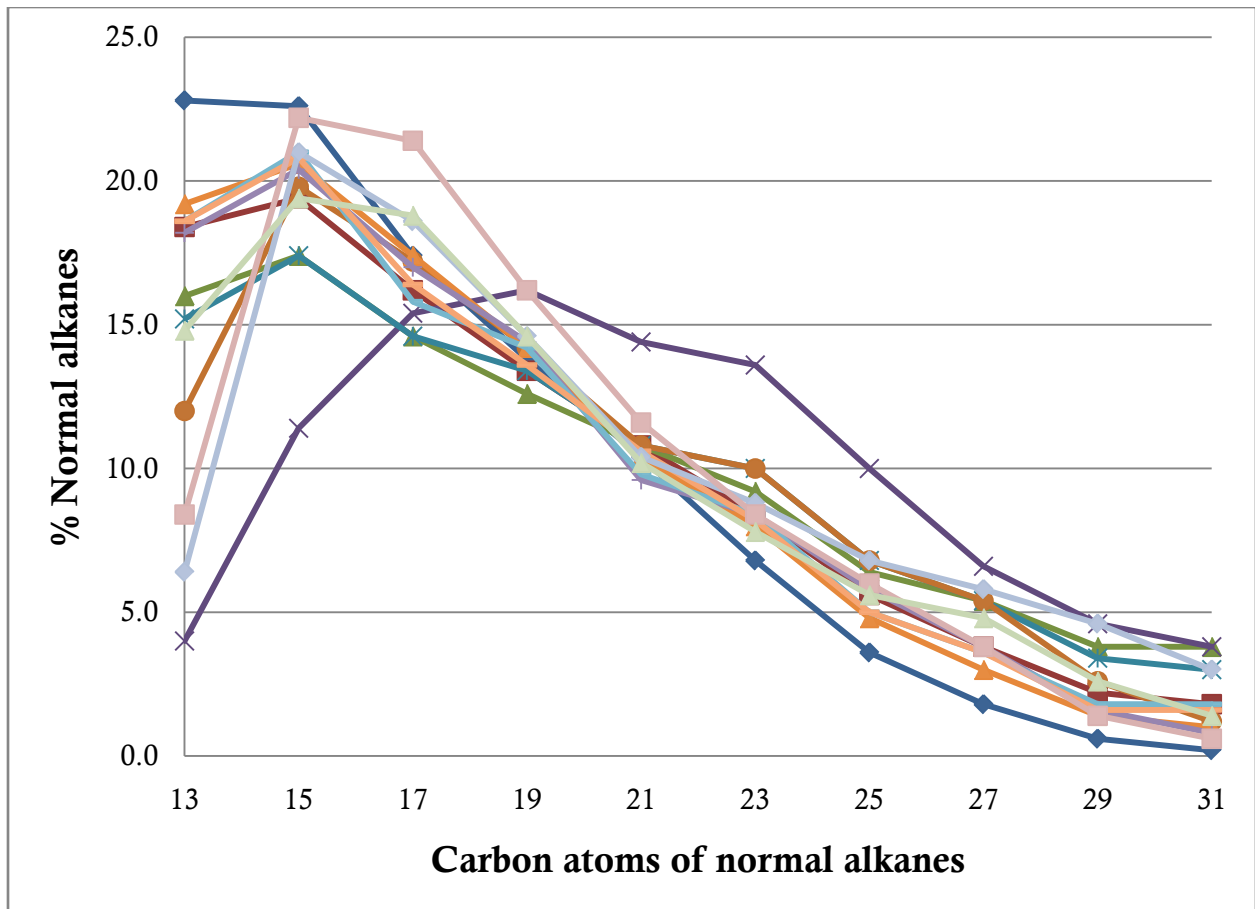


Figure 3.6: *n*-alkane distributions of non-biodegraded oil samples from the Santa Barbara Basin.

### 3.2.9 C<sub>27</sub>-C<sub>28</sub>-C<sub>29</sub> steranes

The C<sub>27</sub>-C<sub>28</sub>-C<sub>29</sub> steranes ternary diagram is often used to distinguish groups of petroleum from different source organic inputs and their depositional environment. Steranes inherited directly from land plants, animals, and algae are 20R epimers of the C<sub>27</sub>, C<sub>28</sub>, C<sub>29</sub>, and C<sub>30</sub> steranes. Relative proportions of the C<sub>27</sub>-C<sub>29</sub> steranes in organisms relate to their specific environments. When majority of sterane in oil is C<sub>29</sub> compared to C<sub>27</sub> and C<sub>28</sub>, it may indicate terrestrial or land plant inputs. Higher proportions of C<sub>27</sub> and C<sub>28</sub> in oils can indicate that their source rocks were deposited in marine and lacustrine environments with mainly algae inputs, respectively. All these parameters can be measured on *m/z* 217 mass chromatogram (Moldowan, *et al.*, 1985).

### Results

High concentrations of C<sub>27</sub> compared to C<sub>28</sub> and C<sub>29</sub> of most oil samples from the San Joaquin Basin (Figure 3.7) may suggest that the source rocks' depositional environments are

estuarine with generally plankton and marine algae inputs, and have occasional inputs from terrestrial organisms.

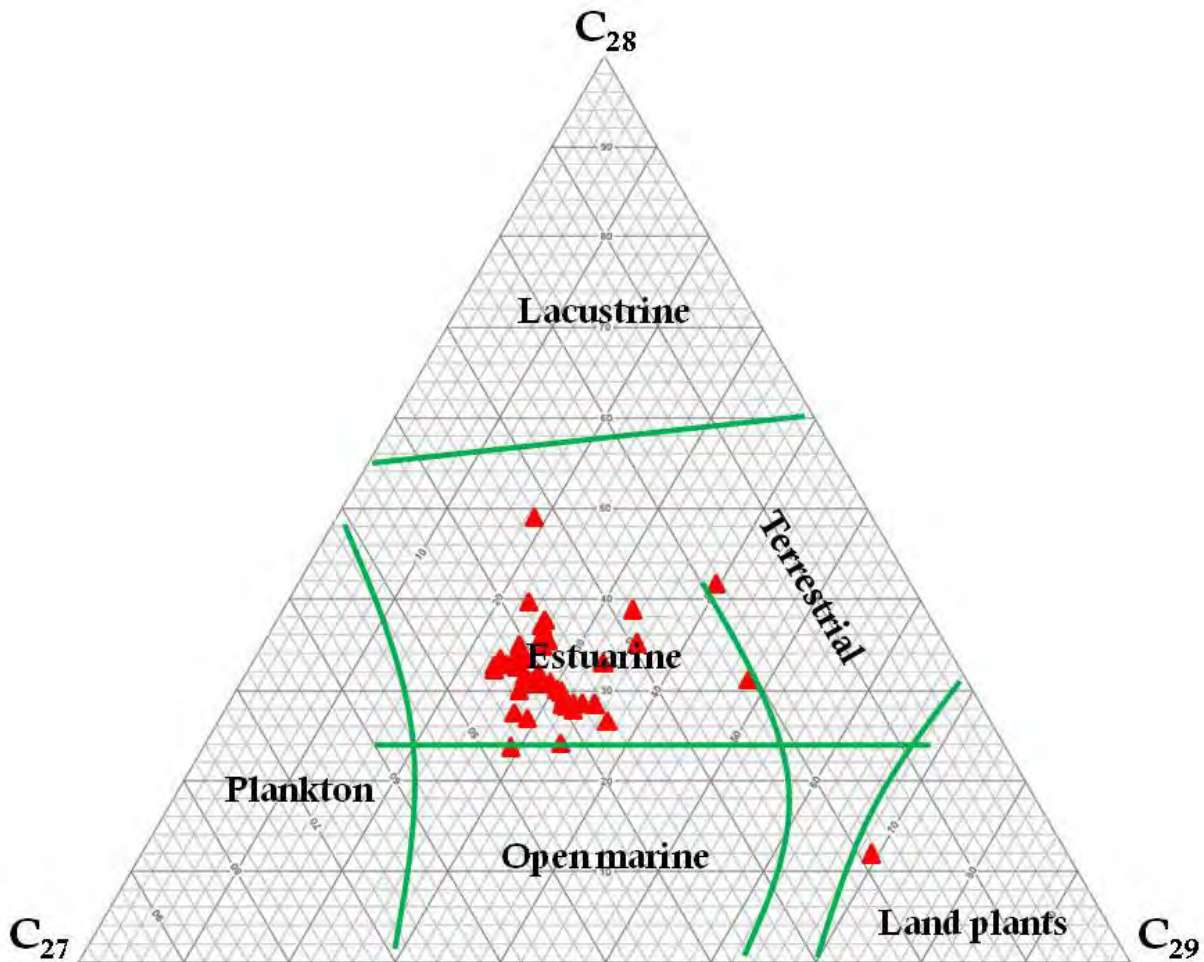


Figure 3.7:  $C_{27}$ - $C_{28}$ - $C_{29}$  steranes ternary diagrams of oils from the San Joaquin Basin.

For the oil samples from the Santa Barbara Basin, the relative proportions of  $C_{27}$ ,  $C_{28}$ , and  $C_{29}$  steranes (Figure 3.8) indicate that the source rocks' depositional environments are estuarine, the same as those of the San Joaquin Basin. Observably, the Santa Barbara Basin's source rocks have relatively more plankton and marine algae inputs which suggest that these source rocks were deposited in deeper marine and further from the continent than the San Joaquin Basin's source rocks.

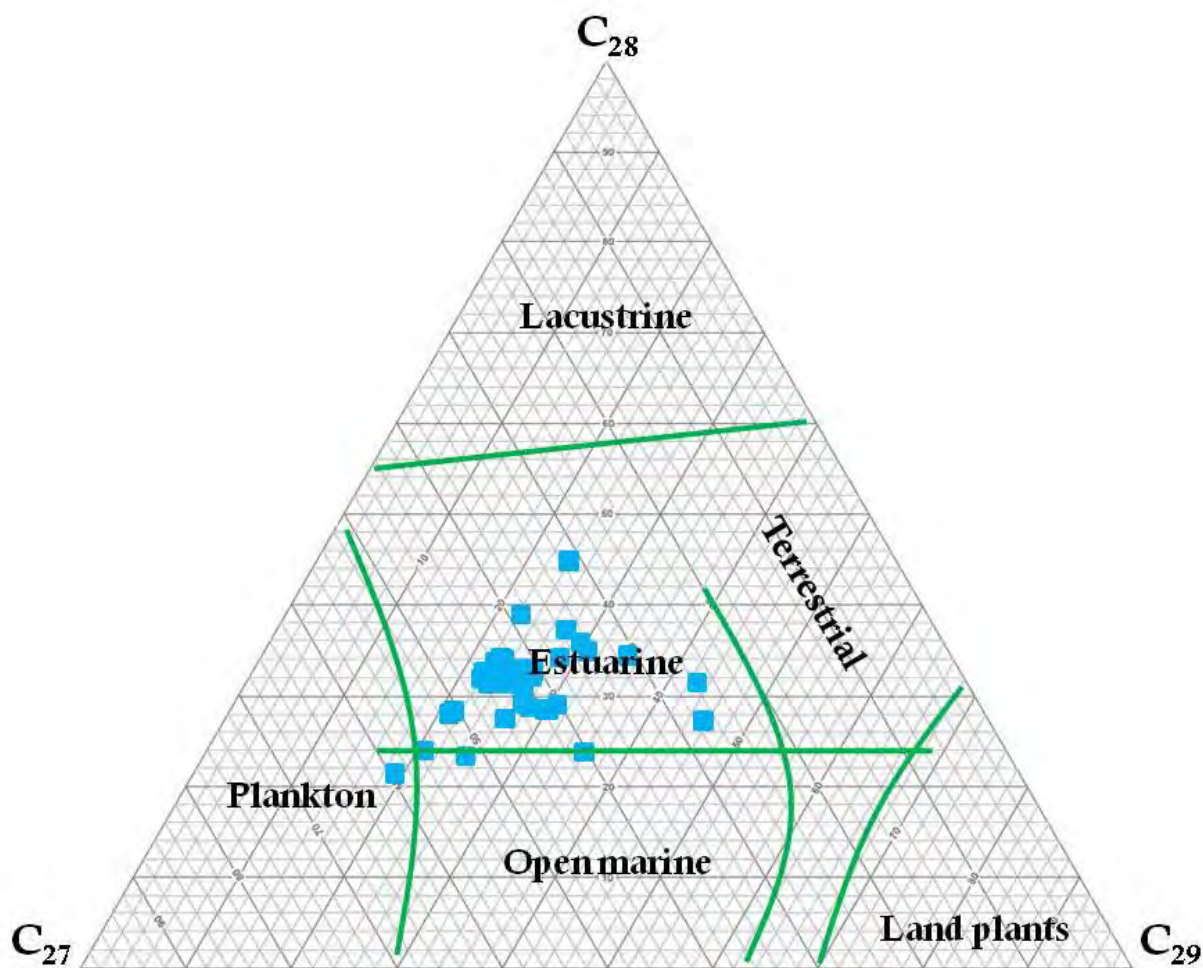


Figure 3.8:  $C_{27}$ - $C_{28}$ - $C_{29}$  steranes ternary diagrams of oils from the Santa Barbara Basin.

### 3.2.10 $C_{26}$ - $C_{27}$ - $C_{28}$ triaromatic steroids

Similar to the  $C_{27}$ - $C_{28}$ - $C_{29}$  steranes, the  $C_{26}$ - $C_{27}$ - $C_{28}$  triaromatic steroids ternary diagram can also be used to discriminate source organic inputs and depositional environment of the source rocks generating petroleum. High concentrations of  $C_{28}$  triaromatic steroids compared to  $C_{26}$  and  $C_{27}$  may indicate mostly land plant inputs in terrestrial environments. When greater proportions of triaromatic steroids are  $C_{26}$  and  $C_{27}$ , they may suggest marine and lacustrine environments with predominant algae inputs. These compounds can be investigated on  $m/z$  231 mass chromatogram in aromatic hydrocarbon fractions. The triaromatic steroids ternary diagram is much more reliable than the sterane ternary diagram because triaromatic steroids are more thermally stable than steranes and are not readily lost to biodegradation (Peters, *et al.*, 2005).

## Result

High concentrations of  $C_{26}$  compared to  $C_{27}$  and  $C_{28}$  of all oil samples from the San Joaquin Basin (Figure 3.9) may imply that the source rocks' depositional environments are estuarine with mainly input from plankton and marine algae with less contribution from terrestrial organism.

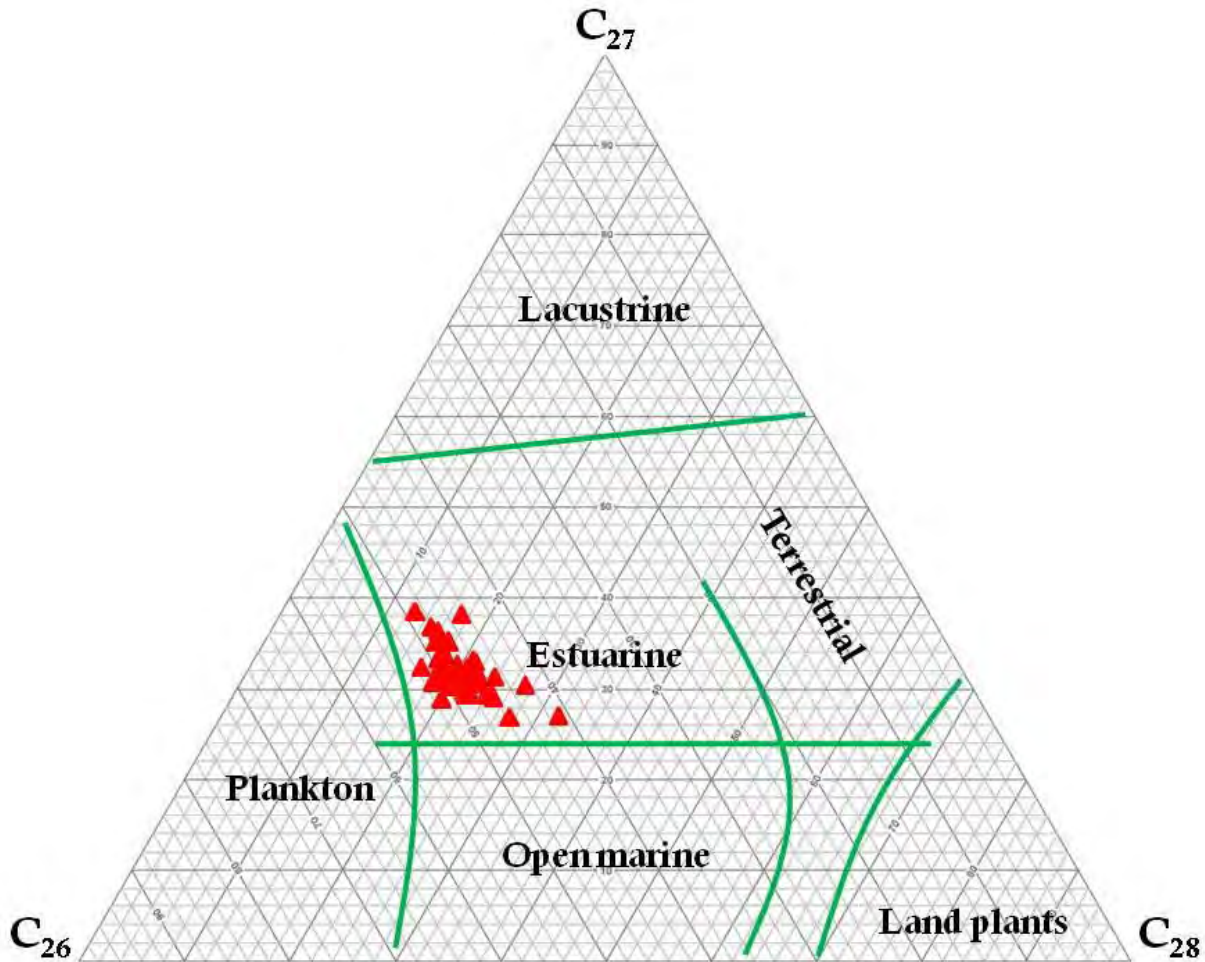


Figure 3.9:  $C_{26}$ - $C_{27}$ - $C_{28}$  triaromatic steroids ternary diagrams of oils from the San Joaquin Basin.

Similar to oils from the San Joaquin Basin, the relative concentrations of  $C_{26}$ ,  $C_{27}$ , and  $C_{28}$  triaromatic steroids (Figure 3.10) suggest that the depositional environments of the source rocks are an estuarine as same as those of the San Joaquin Basin. Noticeably, the Santa Barbara Basin's source rocks have relatively more plankton and marine algae inputs which may indicate that these source rocks were deposited in deeper conditions and further from the continent than the San Joaquin Basin's source rocks.



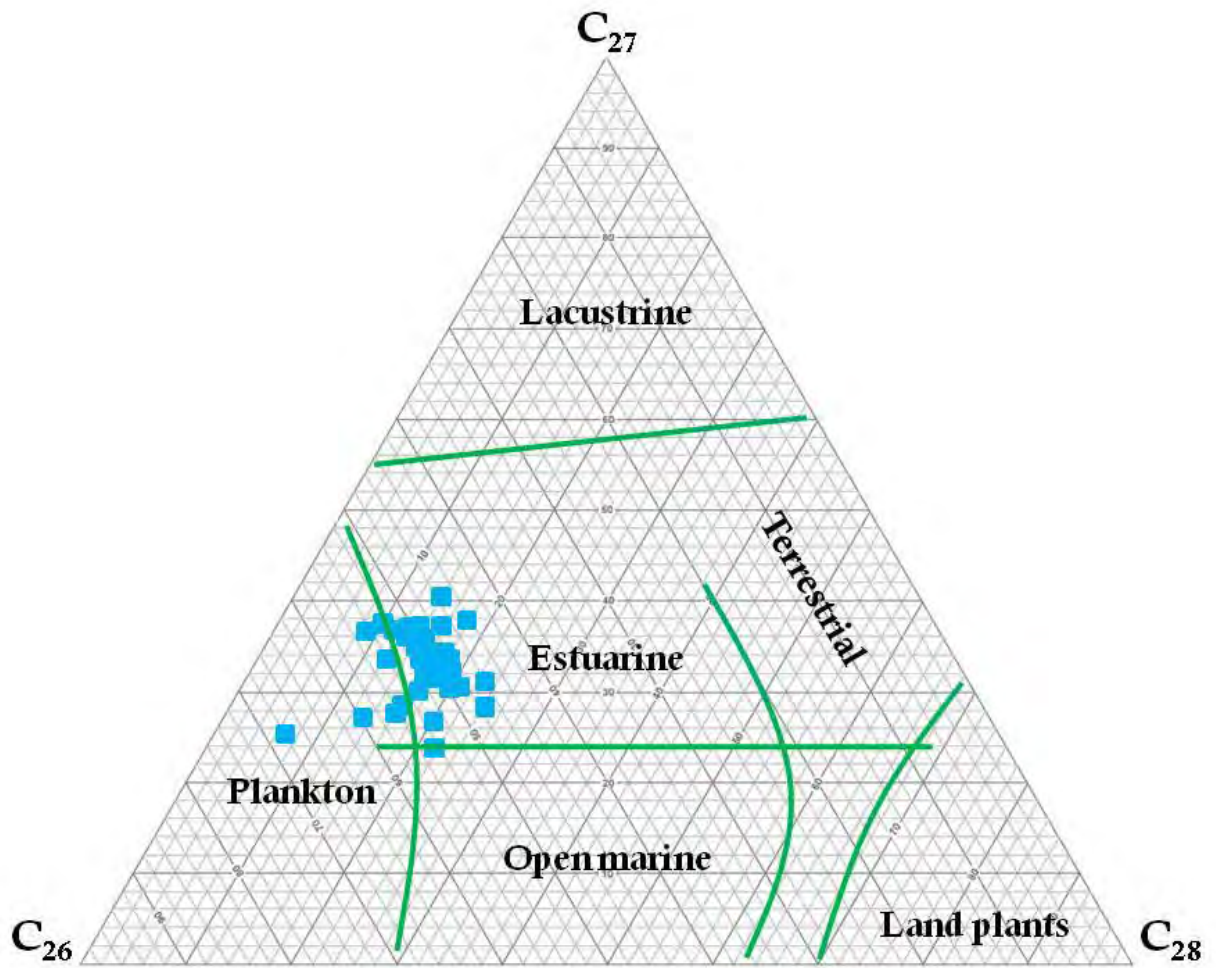


Figure 3.10:  $C_{26}$ - $C_{27}$ - $C_{28}$  triaromatic steroids ternary diagrams of oils from the Santa Barbara Basin.

## CHAPTER IV

### DISCUSSION, CONCLUSION AND RECOMMENDATION

#### 4.1 Discussion

All oil samples from the San Joaquin and Santa Barbara Basins were analyzed by using the geochemical techniques in order to discover possible previously overlooked cracked oil inputs from deeper sources composing of high diamondoid concentrations and to evaluate the biomarker data in terms of types of oil, maturity levels, depositional environment, source of organic inputs, and biodegradation. In this research, many parameters acquired from oil sample extracts are used to accomplish all these prospects.

Diamondoid-biomarker method (Dahl, *et al*, 1999) is an indicator used for identifying types of oil, and cracked oil inputs from deeper sources. The result suggests that both basins likely have important contributions from both shallow and deep sources because most of the samples are mixed oil containing slightly to extremely cracked sources. The types of oil can be classified into 4 major groups: (1) moderate to high maturity uncracked oils, (2) slightly cracked oils mixed with high maturity uncracked oils, (3) extremely cracked oils mixed with high maturity uncracked oils, and (4) extremely cracked oil mixed with very low maturity uncracked oil.

Many parameters are used to determine the maturity levels including  $T_s/(T_s+T_m)$  ratio and homohopane isomerizations. The results from these parameters suggest that oil samples from both basins are of relatively moderate to high maturity (nearly reach the peak of oil window).

The ternary diagrams of  $C_{27}$ - $C_{28}$ - $C_{29}$  steranes and  $C_{26}$ - $C_{27}$ - $C_{28}$  triaromatic steroids are important parameters to specify the depositional environments and source inputs. The results indicate that the San Joaquin and Santa Barbara Basins' source rocks were deposited in shallow marine environments which have dominant algae and plankton inputs with occasional input of land plants. These results are supported by  $Pr/Ph$ ,  $Pr/nC_{17}$ , and  $Ph/nC_{18}$  ratios and  $n$ -alkane distributions. Gammacerane and  $C_{35}$  homohopane can be found in every oil sample which may imply that the source rocks were deposited in anoxic to sub-oxic conditions or in hypersaline environments.

Biodegradation can be examined on hydrocarbon distributions in GC-FID chromatograms. Based on Peters and Moldowan (1993) ranking system, the samples from both basins are varied in biodegradation rank ranging from 0-8.

## 4.2 Conclusion

### 4.2.1 Cracked oils' platform

Cracked oils in this research can be discriminated by using diamondoid-biomarker method. Many oil platforms of the San Joaquin and Santa Barbara Basins reserve oils with significantly high diamondoid concentrations. Oils with 10 ppm of diamondoids were classified as intensely cracked oils which are very interesting to study. Intensely cracked oils found in these platforms as shown in Table 4.1.

San Joaquin Basin	Santa Barbara Basin
F&I Well	Platform Holly
Oil City Field, Fresno	Ojai Silverthread
Old Joel Flat, Petrolia Hidden Valley	Platform B
Coalinga Oil Field	

Table 4.1: Intensely cracked oils' platform of the San Joaquin and Santa Barbara Basins.

### 4.2.2 Types of oil

The diamondoid-biomarker method is also used to categorize oils of both basins. Three and four types of oil can be classified from the San Joaquin and Santa Barbara Basins' oils, respectively as shown in Figure 4.1.

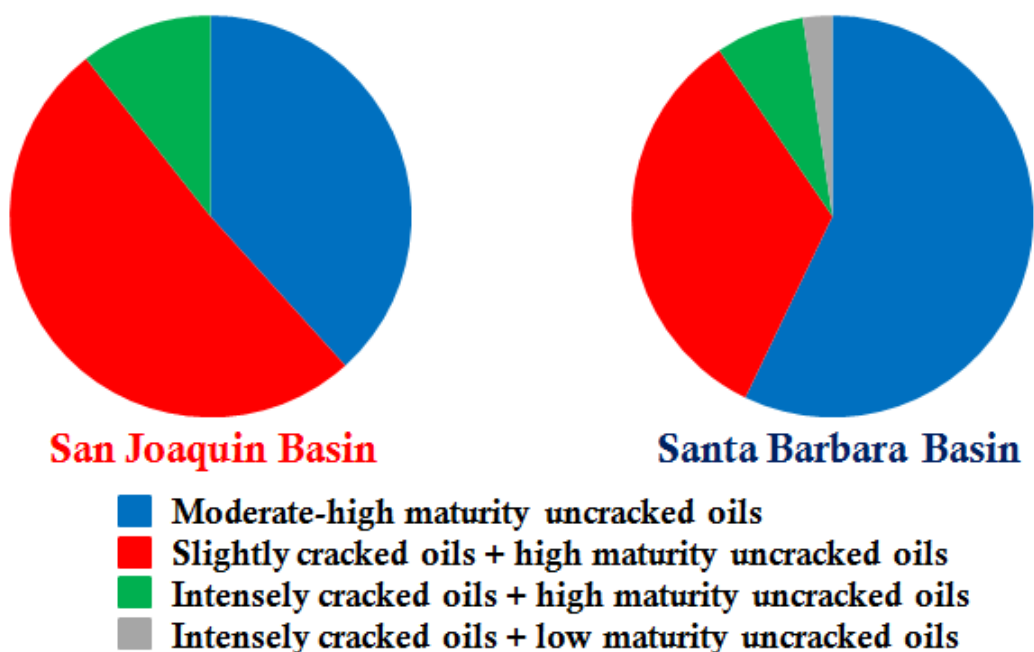


Figure 4.1: Pie charts showing the types of oil of the San Joaquin and Santa Barbara Basins.

### 4.2.3 Maturity levels

Ts/(Ts+Tm) ratio and homohopane isomerization ratios suggest that source rock generating oils in these two basins are of relatively moderate to high maturity and nearly reach the peak of the oil generative window (Figure 4.2). *N*-alkane distributions may also suggest the same level of maturity but they are possibly affected by source organic inputs. Therefore, they are not as useful to determine maturity levels in this research.

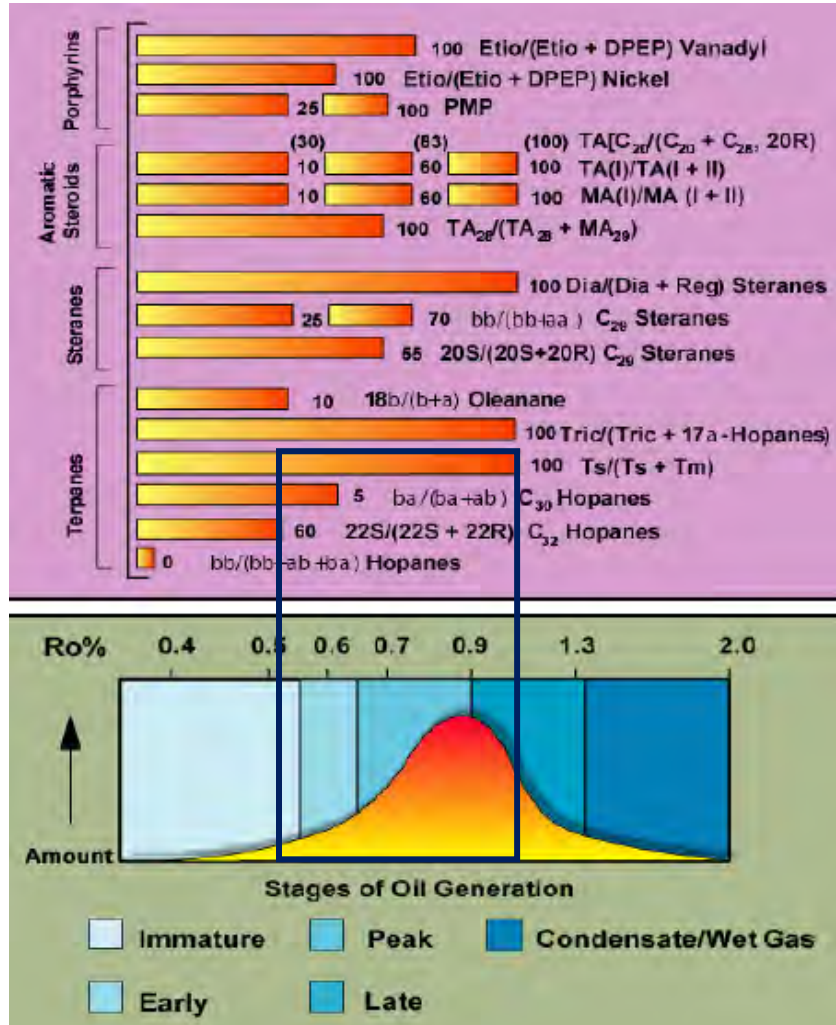


Figure 4.2: Biomarker parameters respond in different maturity levels. Parameters shown include Ts/(Ts+Tm) ratio and homohopane isomerization ratios used in this research (Peters *et al.*, 2005).

### 4.2.4 Depositional environment and source inputs

Biomarker parameters of oil samples from the San Joaquin and Santa Barbara Basins which were analyzed indicate that their source rocks were deposited in hypersaline marine with very low oxygen (as shown by appearance of gammacerane and C<sub>35</sub> homohopane, and *n*-alkane



distributions maximizing  $C_{15}$ ,  $C_{17}$  and  $C_{19}$ ). The organic matter inputs were mainly derived from algae and plankton with occasional land plants which may suggest that the San Joaquin and Santa Barbara Basins source rocks were likely deposited in continental shelf and slope, respectively but the result may still have some uncertainties due to lacking of oil-source correlation study. When comparing to their lithostratigraphy, these major source rocks should be Tertiary in age and other source rocks deposited deeper in Cretaceous time may be the sources contributing to oils with high diamondoid concentrations.

#### 4.2.5 Biodegradation

Hydrocarbon distributions were investigated to determine biodegradation level of oil samples from the San Joaquin and Santa Barbara Basins. It can be noticed that oil samples from the Santa Barbara Basin were more severely biodegraded than oil samples from the San Joaquin Basin as shown in Figure 4.3 because they are mostly seeps.

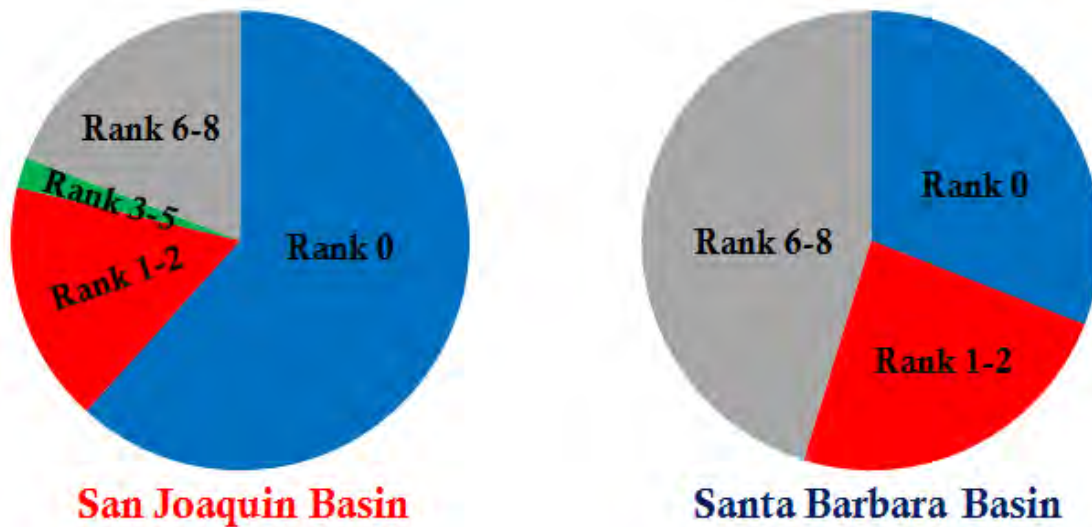


Figure 4.3: Pie charts showing proportions of oils with different biodegradation ranks (based on Peters and Moldowan, 1993) of oil samples from the San Joaquin and Santa Barbara Basins.

#### 4.3 Recommendation

- 1) Analyzing more non-biodegraded oil samples from the San Joaquin and Santa Barbara Basins because biodegradation can affect some parameters.
- 2) Analyzing more biomarker parameters in oil samples from these two basins and studying more oil-source correlation.

## REFERENCES

- Albrecht, P., Vandenbroucke, M., and Mandengue, M., 1976. Geochemical studies on the organic matter from the Douala Basin (Cameroon). Evolution of the extractable organic matter and the formation of petroleum. *Geochimica et Cosmochimica Acta*, 40, 791–799.
- Chung, H.M., Walters, C.C., Buck, S., and Bingham, G., 1998. Mixed signals of the source and thermal maturity for petroleum accumulations from light hydrocarbons: an example of the Beryl Field. *Organic Geochemistry*, 29, 381–396.
- Churley, M. Prest, H., Zinniker, D.A., and Blatt, C., 2009. Enhanced sensitivity for biomarker characterization in petroleum using triple quadrupole GC-MS and backflushing. **Application Notes**, Agilent Technologies.
- Dahl, J.E. Moldowan, J.M., Peters, K.E., Claypool, G.E., Rooney, M.A., Michael, G.E., Mello, M.R., and Kohnen, M.L., 1999. Diamondoid hydrocarbons as indicators of oil cracking. *Nature*, 399, 54-57.
- Dahl, J.E., Moldowan, J.M., Peters, K.E., and Mello, M.R., 1998. Diamondoid hydrocarbons as indicators of thermal maturity and oil-cracking. Abstract, American Association of Petroleum, *Geologists Bulletin*. 82, 1883–1984.
- DeCourten, F., 2006. **Geology of Southern California**, Department of Earth Science Sierra College.
- Farrimond, P., Taylor, A., and Telnæs, N., 1998. Biomarker maturity parameters: the role of generation and thermal degradation. *Organic Geochemistry*, 1981, Chichester, J. Wiley, New York, 675-683.
- Galloway, J.M., 2009, **Santa Barbara-Ventura Basin Province**, Bureau of Ocean Energy Management, Regulation and Enforcement, 20 pp.
- Grice, K., Alexander, R., and Kagi, R.I., 2000, Diamondoid hydrocarbon ratios as indicators of biodegradation in Australian crude oils. *Organic Geochemistry*, 31, 67-73.
- Hunt, J.M., 1996. **Petroleum Geochemistry and Geology**, 2<sup>nd</sup> Edition. Freeman. 743 pp.
- Hunt, J.M., Whelan, J.K., and Huc, A.Y., 1980. Genesis of petroleum hydrocarbons in marine sediments. *Science*, 209, 403–404.

- Johnson, C.L. and Graham, S.A., 2007. Middle Tertiary stratigraphic sequences of the San Joaquin Basin, California. United States Geological Survey. **Petroleum Systems and Geologic Assessment of Oil and Gas in the San Joaquin Basin Province, California**, 18 pp.
- Lillis, P.G. and Magoon, L.B., 2004. Oil-oil correlations to establish a basis for mapping petroleum systems, San Joaquin Basin, California. United States Geological Survey. **Open-File Report**, 2004-1037, 49 pp.
- Lorenson, T.D. Hostettler, F.D., Rosenbauer, R.J., Peters, K.E., Dougherty, J.A., Kvenvolden, K.A., Gutmacher, C.E., Wong, F.L., and Normark, W.R., 2009. Natural offshore oil seepage and related tarball accumulation on the California coastline-Santa Barbara Channel and the southern Santa Maria Basin; source identification and inventory. **Open-File Report**, 2009-1225, 119 pp.
- Mackenzie, A.S., Patience, R.L., and Maxwell, J.R., 1980. Molecular parameters of maturation in the Toarcian shales, Paris Basin, France. Changes in the configuration of acyclic isoprenoid alkanes, steranes, and triterpanes. **Geochimica et Cosmochimica Acta**, 44, 1709–1721.
- Magoon, L.B. and Dow, W.G., 1994. The petroleum system from source to trap. **AAPG Memoir**, 60, 644 pp.
- Mansoori, G.A., 2007. Diamondoid molecules. **Advances in Chemical Physics**, 136, 207-258.
- Minor, S.A. Kellogg, K.S., Stanley, R.G., Stone, C.L., Paul, C.L., Powell, C.L., Gurrola, L.D., Selting, A.J., and Brandt, T.R., 2003. Preliminary Geologic Map of the Santa Barbara Coastal Plain Area, Santa Barbara County, California. United States Geological Survey. **Open File Report**, 02-136. Digital version 1.1, compiled at a scale of 1:24000.
- Moldowan, J.M., Dahl, J.E., Huizinga, B.J., Fago, F.J., Hickey, L.J., Peakman, T.M., and Taylor, D.W., 1994. The molecular fossil record of oleanane and its relation to angiosperms. **Science**, 265, 768-771.
- Moldowan, J.M., Seifert, W.K., and Gallegos, E.J., 1985. Relationship between petroleum composition and depositional environment of petroleum source rocks. **American Association of Petroleum Geologists Bulletin**, 69, 1255-1268.
- Peters, K.E. and Fowler, M.G., 2002. Applications of petroleum geochemistry to exploration and reservoir management. **Organic Geochemistry**, 33, 5-36.

- Peters, K.E. and Moldowan, J.M., 1993. **The Biomarker Guide: Interpreting molecular fossils in petroleum and ancient sediments**, Englewood cliffs, New Jersey, Prentice Hall, 363 pp.
- Peters, K.E., Walters, C.C., Moldowan, J.M., 2005. **The Biomarker Guide**, Volumes 1 & 2, Biomarkers and Isotopes in Petroleum Exploration and Earth History. The University Press, Cambridge, 1155 pp.
- Scheirer, A.H. and Magoon, L.B., 2007. Age, distribution, and stratigraphic relationship of rock units in the San Joaquin Basin Province, California. **United States Geological Survey Professional Paper**, 1713, Chapter 5, 107 pp.
- Seifert, W.K. and Moldowan, J.M., 1980. The effect of thermal stress on source-rock quality as measured by hopane stereochemistry. **Physics and Chemistry of the Earth**, 12, 229–237.
- Seifert, W.K. and Moldowan, J.M., 1986. Use of biological markers in petroleum exploration. **Biological Markers in the Sedimentary Record**, Amsterdam, Elsevier, 261-290.
- Shanmugam, G., 1985. Significance of coniferous rain forest and related organic matter in generating commercial quantities of oil, Gippsland basin, Australia. **AAPG Bulletin**, 69, 1241-1254.
- Tasa Graphic Arts, Inc., 2009. **San Andreas Fault System**, Available from: [http://tasaclips.com/illustrations/San\\_Andreas\\_Fault\\_System.jpg](http://tasaclips.com/illustrations/San_Andreas_Fault_System.jpg).
- Tissot, B.P. and Welte, D.H., 1978. Petroleum formation and occurrence: a new approach to oil and gas exploration. **Springer-Verlag**, New York.
- Thompson, K.F.M., 1983. Classification and thermal history of petroleum based on light hydrocarbons. **Geochimica et Cosmochimica Acta**, 47, 303–316.
- Volkman, J.K., 1988. Biological marker compounds as indicators of the depositional environments of petroleum source rocks, in Fleet, A.J., Kelts, K., and Talbot, A.R. (editor). **Lacustrine Petroleum Source Rocks**, Oxford, Blackwell, 103-122.
- Wei, Z., Moldowan, J.M., Zhang, S., Hill, R., Jarvie, D.M., Wang, H., Song, F., and Fago, F.J., 2007. Diamondoid hydrocarbons as a molecular proxy for thermal maturity and oil cracking: Geochemical models from hydrous pyrolysis. **Organic Geochemistry**, 38, 227-249.
- Wilson, A.M., Graven, G., and Boles, J.R., 1999. Paleohydrogeology of the San Joaquin Basin, California. **Geological Society of America Bulletin**, 111, no. 3, 432-449.

## APPENDIX

Appendix I: Biodegradation ranking

Appendix II: Tectonic evolution of the San Joaquin Basin

Appendix I  
Biodegradation ranking

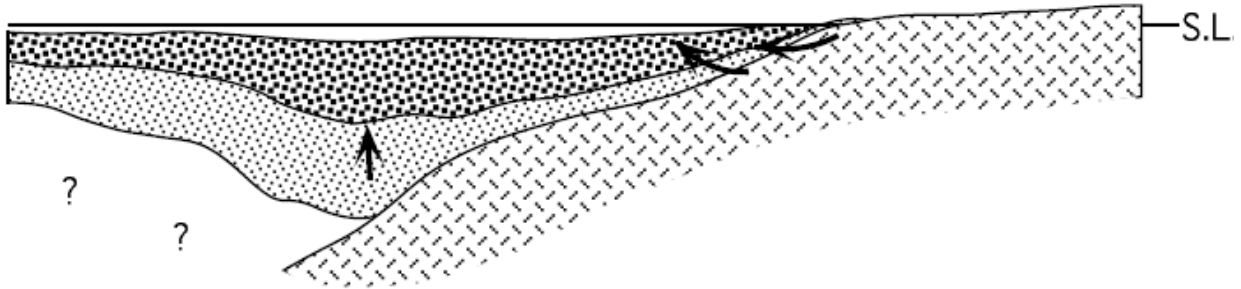
Biodegradation Ranking	N-alkanes	Isoprenoids	Steranes	Hopanes	Diasteranes	Aromatic steroids
1	↔					
2	↔					
3	↔					
4	↔					
5	↔					
6	↔			↔		
7	↔					
8	↔					
9	↔					
10	↔					

Table A-1: Biodegradation ranking based on Peters and Moldowan (1993), double arrow means disappear.

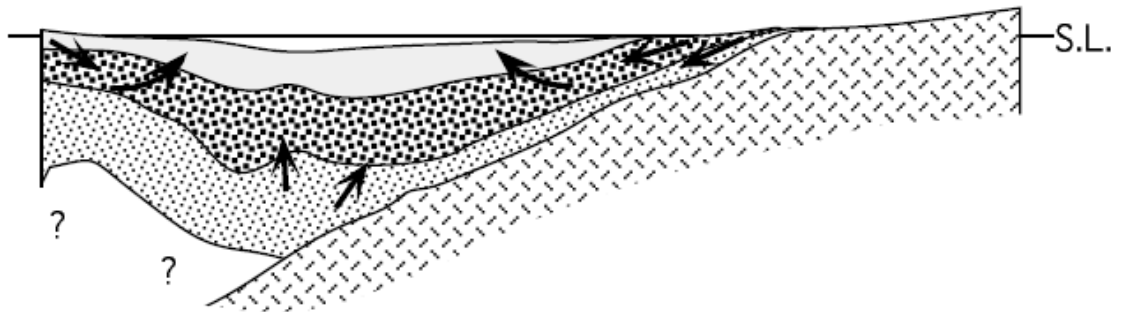
Appendix II

Tectonic evolution of the San Joaquin Basin

Late Miocene, 5-10 Ma



Pliocene, 2 Ma



Recent

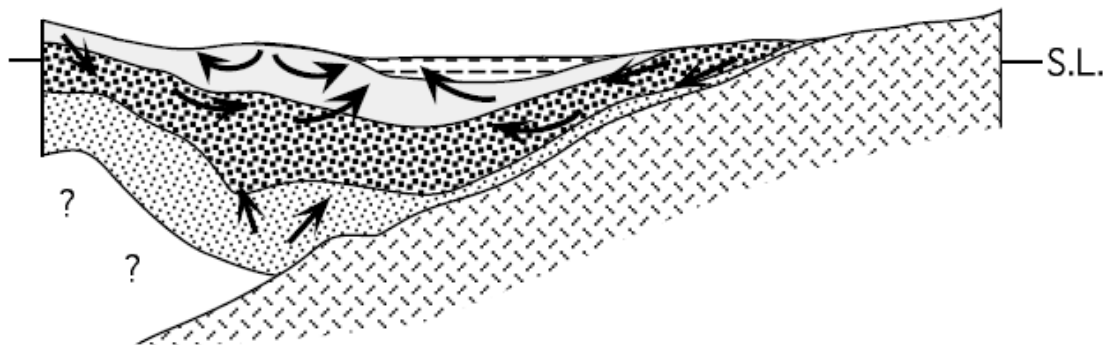


Figure A-1: Tectonic evolution of the San Joaquin Basin. Topography- and compaction-driven flow are shown as arrows. The active tectonics include uplift of the Sierra Nevada beginning 5–10 Ma, the rise of the Coast Ranges above sea level (S.L.) and the last marine regression starting on 2 Ma. Dashed, gray, dark stippled, light stippled, and hachured units represent Post-Pliocene, Pliocene, Miocene, Pre-Miocene, and Sierran rocks, respectively (Wilson *et al.*, 1999).